

Toolkit for staggered $\Delta S = 2$ matrix elements

Jongjeong Kim,¹ Weonjong Lee,^{1,*} Jaehoon Leem,¹ Stephen R. Sharpe,^{2,†} and Boram Yoon³
(SWME Collaboration)

¹*Lattice Gauge Theory Research Center, FPRD, and CTP,
Department of Physics and Astronomy, Seoul National University, Seoul, 151-747, South Korea*

²*Physics Department, University of Washington, Seattle, WA 98195-1560, USA*

³*Los Alamos National Laboratory, MS B283, P.O. Box 1663, Los Alamos, NM 87545, USA*

(Dated: May 17, 2022)

A recent numerical lattice calculation of the kaon mixing matrix elements of general $\Delta S = 2$ four-fermion operators using staggered fermions relied on two auxiliary theoretical calculations. Here we describe the methodology and present the results of these two calculations. The first concerns one-loop matching coefficients between staggered lattice operators and the corresponding continuum operators. Previous calculations with staggered fermions have used a non-standard regularization scheme for the continuum operators, and here we provide the additional matching factors needed to connect to the standard regularization scheme. This is the scheme in which two-loop anomalous dimensions are known. We also observe that all previous calculations of this operator matching using staggered fermions have overlooked one matching step in the continuum. This extra step turns out to have no impact on three of the five operators (including that relevant for B_K), but does affect the other two operators. The second auxiliary calculation concerns the two-loop renormalization group (RG) evolution equations for the B -parameters of the $\Delta S = 2$ operators. For one pair of operators, the standard analytic solution to the two-loop RG equations fails due to a spurious singularity introduced by the approximations made in the calculation. We give a non-singular expression derived using analytic continuation, and check the result using a numerical solution to the RG equations. We also describe the RG evolution for “golden” combinations of B -parameters, and give numerical results for RG evolution matrices needed in the companion lattice calculation.

PACS numbers: 11.15.Ha, 12.38.Gc, 12.38.Aw
Keywords: lattice QCD, B_K , CP violation

I. OVERVIEW

There have been several recent lattice calculations of the kaon mixing matrix elements of all $\Delta S = 2$ operators appearing in a general theory of physics beyond the standard model (BSM)[1–6]. These matrix elements are needed in order to use the experimental results for ε_K and ΔM_K to constrain the parameters of models of new physics. As members of the SWME collaboration, we have been involved in a calculation using improved staggered fermions, which recently presented results in Refs. [3, 5]. These results rely on two auxiliary theoretical calculations, and the purpose of this paper is to present the details and results of these calculations.

The first auxiliary calculation concerns the matching between the continuum operators whose matrix elements we desire and the lattice operators whose matrix elements we calculate. We use one-loop perturbative matching. The requisite one-loop calculations have been done in Ref. [7], but only using a non-standard continuum scheme for defining four-fermion operators. This scheme, introduced in Ref. [8], has attractive properties under Fierz transformations, but has not been adopted in the continuum literature. Instead, the standard continuum scheme

is that used in Ref. [9] to calculate the two-loop anomalous dimensions for the complete set of $\Delta S = 2$ operators. This scheme differs from that of Ref. [8] in the choice of evanescent operators. Since we need the two-loop anomalous dimensions in order to evolve lattice results to a common scale, it is necessary to match the lattice operators to the standard continuum scheme. Thus we have augmented the results of Ref. [7] by calculating the matching factor between the two continuum schemes.

Undertaking this relatively straightforward task, we have uncovered a conceptual error in previous staggered perturbative matching calculations for four-fermion operators [7, 10, 11]. It turns out that the matching factors obtained in these works connect the lattice operators to continuum operators which are non-standard not only because of the choice of scheme just described, but also because of an additional finite correction. Technically, this arises because an additional continuum-to-continuum matching step is required. In general this leads to a correction beginning at one-loop order. Since this point is of more general interest for applications using staggered fermions, we explain it in some detail.

It turns out that the additional matching corrections vanish for three of the five operators which arise in a general BSM theory. In particular, previous results for the standard-model B_K operator are unaffected.

The second auxiliary calculation concerns the renormalization group (RG) running in the continuum. Our lattice calculation needs RG evolution to convert results

* E-mail: wlee@snu.ac.kr

† E-mail: srsharpe@uw.edu

obtained at the lattice scale $1/a$ to a standard scale such as 2 GeV. Although this might appear to be a standard calculation, there are two complications which arise. First, the standard expressions for two-loop running break down for one pair of operators, due to a spurious singularity. In this case one can either use the analytic continuation method of Ref. [12], or simply solve the RG equations numerically. We have compared these approaches, and present numerical results for the evolution matrices. The second complication is that, in our lattice calculation, we make use of particular “golden” ratios or products of B -parameters which are chosen to have simpler chiral extrapolations [13, 14]. Here we present the formulae for RG evolution of these combinations.

A further reason for presenting our RG running factors is that there is some disagreement between the results for BSM matrix elements of our work and those of Refs. [1, 2, 4, 6]. Thus it is useful to present the technical details of our work so as to facilitate a more thorough comparison.

This paper is organized as follows. In Sec. II, we recall the relevant $\Delta S = 2$ operators and define the corresponding B -parameters. The method for calculating the one-loop matching factors is described in Section III, and final results are presented. The issues arising in RG evolution are described in Section IV. We include three appendices. Appendix A provides the technical details of the calculation of the matching factors, Appendix B collects results for anomalous dimensions, and Appendix C gives numerical results for evolution kernels.

II. CONTINUUM $\Delta S = 2$ OPERATORS AND B -PARAMETERS

The $\Delta S = 2$ effective Hamiltonian has the general form

$$\mathcal{H}_{\text{eff}}^{\Delta S=2} = \sum_i C_i(\mu) Q_i(\mu), \quad (1)$$

where the Q_i form a basis of $\Delta S = 2$ four-fermion operators, and the C_i are Wilson coefficients. This form holds both in the standard model (SM) and in a general BSM theory, and arises after heavy particles are integrated out. Contributions from operators of higher dimension are neglected. Both C_i and Q_i depend on the renormalization scale μ , as is displayed explicitly. They also have an implicit dependence on the regularization scheme used to define the operators. This could either be a continuum scheme or some form of lattice regularization. The scheme and scale dependence cancels in \mathcal{H}_{eff} , and using this one can determine how the C_i depend on the scheme and on μ . Determining the relationship between the C_i in different schemes and at different scales is the focus of this paper.

We first consider the form of the operators that appear in continuum regularization. These will be given a superscript “Cont”. In the SM, the left-handed couplings of the W -boson imply that only a single operator

has a non-vanishing Wilson coefficient, namely that with “left-left” spin structure:

$$Q_1^{\text{Cont}} \equiv Q_K^{\text{Cont}} = [\bar{s}^a \gamma_\mu L d^a][\bar{s}^b \gamma_\mu L d^b]. \quad (2)$$

Here $L = (1 - \gamma_5)$, a and b are color indices, and repeated indices are summed. We work in Euclidean space throughout. In a general BSM theory, four other operators appear in addition to Eq. (2). These can be chosen to be

$$Q_2^{\text{Cont}} = [\bar{s}^a L d^a][\bar{s}^b L d^b], \quad (3)$$

$$Q_3^{\text{Cont}} = [\bar{s}^a \sigma_{\mu\nu} L d^a][\bar{s}^b \sigma_{\mu\nu} L d^b], \quad (4)$$

$$Q_4^{\text{Cont}} = [\bar{s}^a L d^a][\bar{s}^b R d^b], \quad (5)$$

$$Q_5^{\text{Cont}} = [\bar{s}^a \gamma_\mu L d^a][\bar{s}^b \gamma_\mu R d^b], \quad (6)$$

where $R = (1 + \gamma_5)$ and $\sigma_{\mu\nu} = [\gamma_\mu, \gamma_\nu]/2$. This is essentially the basis given in Ref. [9], which we call the “Dirac basis”.¹ A complete definition also requires a choice of basis for the evanescent operators, i.e. those which appear when one extends from 4 to $D = 4 - 2\epsilon$ dimensions. We use the choice of Ref. [9]. This is the scheme in which the two-loop anomalous dimensions have been calculated.

The list of operators given above is, in fact, incomplete. Three more operators can appear—those obtained from $Q_{1,2,3}^{\text{Cont}}$ by interchanging L and R . We do not consider these operators separately because we are ultimately interested in the positive parity parts of all operators, which are the same for both left- and right-handed operators. Only the positive parity parts contribute to the $K^0 - \bar{K}^0$ mixing matrix elements. Furthermore, the matching of the right-handed operators to the corresponding lattice operators involves identical coefficients as for the left-handed operators, and the RG running is also identical.

It is useful in lattice calculations to determine dimensionless B -parameters rather than matrix elements. For the Dirac basis operators, these are

$$B_1 = B_K = \frac{\langle \bar{K}^0 | Q_1^{\text{Cont}} | K^0 \rangle}{N_1 \langle \bar{K}^0 | \bar{s} \gamma_\mu \gamma_5 d | 0 \rangle \langle 0 | \bar{s} \gamma_\mu \gamma_5 d | K^0 \rangle} \quad (7)$$

$$B_i = \frac{\langle \bar{K}^0 | Q_i^{\text{Cont}} | K^0 \rangle}{N_i \langle \bar{K}^0 | \bar{s} \gamma_5 d | 0 \rangle \langle 0 | \bar{s} \gamma_5 d | K^0 \rangle} \quad \text{for } i = 2, 3, 4, 5 \quad (8)$$

where $N_j = \left\{ \frac{8}{3}, \frac{5}{3}, 4, -2, \frac{4}{3} \right\}$ for $j = 1, 2, 3, 4, 5$, respectively. The denominators are obtained using the vacuum

¹ Specifically, our operators are related to those of Ref. [9] by $Q_{2,3}^{\text{Cont}} = 4Q_{1,2}^{SLL}$ and $Q_{4,5}^{\text{Cont}} = 4Q_{2,1}^{LR}$. The factor of four arises because we use $(1 \pm \gamma_5)$ instead of $(1 \pm \gamma_5)/2$ in order to simplify some subsequent results. This factor cancels in suitably defined B -parameters and in anomalous dimensions. We have also reordered the “ LR ” operators.

insertion approximation though only keeping the leading terms in the SU(3) chiral limit. We stress that these B -parameters are simply useful intermediate quantities, with their precise definition being immaterial as long as one uses the same definition throughout.

An alternative to the Dirac basis is the ‘‘SUSY basis’’ of Ref. [15]:

$$\mathcal{O}_1^{\text{Cont}} = Q_1^{\text{Cont}}, \quad (9)$$

$$\mathcal{O}_2^{\text{Cont}} = Q_2^{\text{Cont}}, \quad (10)$$

$$\mathcal{O}_3^{\text{Cont}} = [\bar{s}^a L d^b][\bar{s}^b L d^a], \quad (11)$$

$$\mathcal{O}_4^{\text{Cont}} = Q_4^{\text{Cont}}, \quad (12)$$

$$\mathcal{O}_5^{\text{Cont}} = [\bar{s}^a L d^b][\bar{s}^b R d^a]. \quad (13)$$

This has been used, for example, in the lattice calculations of Refs. [1, 2, 4, 6]. The corresponding B -parameters are defined as in Eqs. (7) and (8), except with $N_3 = -1/3$ and $N_5 = -2/3$. In four dimensions one can relate the two bases using Fierz transformations, while in $D \neq 4$ dimensions the relation involves additional evanescent operators:

$$Q_3^{\text{Cont}} = 4\mathcal{O}_2^{\text{Cont}} + 8\mathcal{O}_3^{\text{Cont}} + \text{evanescent}, \quad (14)$$

$$Q_5^{\text{Cont}} = -2\mathcal{O}_5^{\text{Cont}} + \text{evanescent}. \quad (15)$$

A key point, however, is that the way the SUSY basis operators are defined in Refs. [1, 2, 4, 6] is by using the *four-dimensional* Fierz transform to relate them to the Dirac basis. It is in the latter basis that the evanescent operators are defined and in which RG running is done. This means that the B -parameters in the two bases can be related simply using the $D = 4$ results. In particular, $B_i^{\text{SUSY}} = B_i$ for $i = 1, 2, 4$, and 5, while

$$B_3^{\text{SUSY}} = -\frac{3}{2}B_3 + \frac{5}{2}B_2. \quad (16)$$

The latter result follows from the $D = 4$ relation

$$\mathcal{O}_3^{\text{SUSY}} = \frac{Q_3 - 4Q_2}{8}, \quad (17)$$

obtained by inverting Eq. (14) in $D = 4$.

III. ONE-LOOP MATCHING

As noted in the Introduction, one-loop matching calculations with staggered fermions [7, 10, 11] use different continuum operators than those discussed in the previous section. The difference is twofold: the use of a different basis of evanescent operators and a missing matching step. In this section we describe how to change the previous calculations in order to match to the desired continuum operators. The key is to understand the impact of the extra tastes that come with staggered fermions.

It turns out that the just-mentioned differences in continuum operators have no impact on the one-loop matching factors for the continuum operators Q_1^{Cont} , Q_4^{Cont} and

Q_5^{Cont} . Thus the matching factors for these operators obtained in Ref. [7] are correct. Why this is the case will become clear only when the analysis is complete. Given this result, we couch our discussion in terms of the operators Q_2^{Cont} and Q_3^{Cont} , for which the differences do lead to changes in the matching factors.

A. Staggered Complications

In a lattice calculation with staggered fermions, one must deal with the fact that each lattice field yields four degenerate tastes in the continuum limit. For sea quarks this is done by taking the fourth root of the fermion determinant. This prescription is not controversial in perturbation theory, where it is implemented by dividing each quark loop by a factor of four. In fact, for the matching factors we consider, quark loops do not enter until two-loop order so we will not need this prescription for our one-loop calculation.

For the valence quarks, on the other hand, one must account for the fact that the lattice theory has more degrees of freedom than QCD. This means that, even in the continuum limit (where taste symmetry is restored) the lattice theory is *different* from QCD. In particular, it is necessarily a partially quenched (PQ) theory. Although ‘‘rooting’’ ensures that the β -function agrees with that of QCD, the matching of operators, where rooting is not an option, is more complicated.

To understand this in more detail, consider the matrix element of Q_2^{Cont} [Eq. (3)] between an external kaon and antikaon in QCD. Both particles are destroyed/created by a local, color-singlet operator of the form $\bar{d}^a \gamma_5 s^a$. The matrix element involves two types of Wick contractions, one in which the fields in the external operator are both contracted with the \bar{s} and d in a single bilinear, and the other in which the external fields are contracted with an \bar{s} from one bilinear and a d from the other. In the first type of contraction the color indices form two loops, while in the second they form a single loop. Thus we refer to them respectively as ‘‘two color-loop’’ and ‘‘one color-loop’’ contractions.² At tree-level, where one can work in four dimensions, the one color-loop contraction can be rewritten by doing a Fierz transformation on the

² This classification into two types of contraction holds also in perturbation theory (PT), although the description in terms of color-loops is less appropriate. This is because, in PT, one uses external quark fields with uncontracted Dirac and color indices and having definite momentum rather than pseudoscalar, color-singlet kaon operators. Specifically, one uses $\bar{d}_\alpha^a(p_1) s_\beta^b(p_2) \bar{d}_\gamma^c(p_3) s_\gamma^d(p_4)$ in QCD. One can, however, still group the fields into two $\bar{d}s$ pairs in an unambiguous (although arbitrary) way using the external indices and/or momenta as labels, and then define one and two color-loop contractions relative to those pairings.

operator:

$$Q_2^{\text{Cont}} \stackrel{D=4}{=} -\frac{1}{2}[\bar{s}^a L d^b][\bar{s}^b L d^a] + \frac{1}{8}[\bar{s}^a \sigma_{\mu\nu} L d^b][\bar{s}^b \sigma_{\mu\nu} L d^a]. \quad (18)$$

In this form, the one color-loop contraction now has the fields in each external operator contracted with those in a single bilinear. Note that the Fierz-transformed forms involve the same Dirac structures as in $Q_{2,3}^{\text{Cont}}$, but with color indices contracted differently.

We next consider the analogous operators in the continuum limit of the staggered theory. In this theory we have fields S and D , where upper case is used to indicate that there are four tastes of each of the valence quarks, so that S and D are vectors with an implicit taste index. A possible choice of operator to match with Q_2^{Cont} is then

$$[\bar{S}^a(L \otimes \xi_5)D^a][\bar{S}^b(L \otimes \xi_5)D^b]. \quad (19)$$

Here the second matrix in each tensor product indicates the taste matrix. We have chosen the bilinears to have ‘‘Goldstone’’ taste, since that is what is done in actual lattice calculations, but we stress that the problem we are about to explain occurs for any choice of taste. If we now take the matrix element of this operator between a kaon destroyed by $\bar{D}\gamma_5 \otimes \xi_5 S$ and an antikaon created by an operator of the same form, there will again be two types of Wick contraction. At tree-level, the two color-loop contraction will be the same as that for Q_2^{Cont} in QCD, aside from an overall taste factor of N_T^2 , where $N_T = 4$. (This arises because there are two ‘‘taste-loops’’, in each of which all four tastes can flow.) To evaluate the one color-loop contraction at tree-level we can Fierz-transform the operator so that the contraction involves two taste loops. This now requires simultaneous Fierz transformations on Dirac and taste indices. The former transform as in Eq. (18), while the taste transformation is

$$\xi_5 \cdot \xi_5 \longrightarrow \sum_F \frac{\text{tr}(\xi_5 \xi_F \xi_5 \xi_F)}{N_T^2} \xi_F \cdot \xi_F, \quad (20)$$

with F being summed over all sixteen tastes. Upon contraction with the external kaons of taste ξ_5 , only the $F = 5$ term contributes. This comes with a ‘‘Fierz factor’’ of $\text{tr}\mathbf{1}/N_T^2 = 1/N_T$ as well as the overall factor of N_T^2 . Thus the one color-loop contraction at tree-level is the same that for Q_2^{Cont} in QCD, aside from a taste factor of N_T . We now can see the key problem: the two types of contraction come with *different* taste factors compared to the QCD operator. Thus, even with an overall rescaling, the entire matrix elements cannot match. This is the inevitable consequence of the presence of the additional tastes.

This problem has been recognized since the first calculation of matrix elements using staggered fermions [16], and the solution adopted has been to match Wick contractions rather than operators. This solution is explained in Ref. [17], but, as noted above, is incomplete.

In the next few subsections we give the complete description, which involves a sequence of four matching steps.

B. First Matching Step: QCD to PQQCD

In the first step we match from QCD to a partially quenched extension of QCD in which there are two degenerate valence strange quarks, s_1 and s_2 , and two degenerate valence down quarks, d_1 and d_2 . The sea-quark composition is the same as in QCD, and we consider this theory only in the continuum. In this paper we refer to this specific theory as PQQCD. At this stage there is no taste degree of freedom, so this is *not* the continuum limit of a staggered lattice theory. We regulate this theory using dimensional regularization, using an NDR scheme in which evanescent operators are generalized from QCD to the PQ theory in the simplest way (as discussed below). The reason for introducing this theory is that it allows us to separate the two types of Wick contraction without needing to deal with the complications arising from the additional tastes.

Consider the matrix element in PQQCD of

$$Q_{2,II}^{\text{PQ}} = 2[\bar{s}_1^a L d_1^a][\bar{s}_2^b L d_2^b] \quad (21)$$

between a K_1^0 created by $\bar{d}_1 \gamma_5 s_1$ and a \bar{K}_2^0 destroyed by $\bar{d}_2 \gamma_5 s_2$. This matrix element is identical, diagram by diagram in PT, to the two color-loop Wick contractions of Q_2^{Cont} between an external kaon and antikaon in QCD. The factor of 2 in Eq. (21) is needed because, in QCD, each external operator can be contracted with either bilinear, while in PQQCD this is not possible. Because the matching is with the two color-loop contraction in QCD, we label $Q_{2,II}^{\text{PQ}}$ with the additional subscript II .

This diagram by diagram equality in fact holds much more generally. If one uses the external fields $\bar{d}_\alpha^a(p_1) s_\beta^b(p_2) \bar{d}_\gamma^c(p_3) s_\delta^d(p_4)$ in QCD (with $\alpha - \delta$ Dirac indices), and keeps only the contractions in which the fields with momenta p_1 and p_2 are connected to the same bilinear (so that the fields with momenta p_3 and p_4 are connected to the other bilinear) then the matrix element agrees exactly with that in PQQCD with external fields $\bar{d}_{1,\alpha}^a(p_1) s_{1,\beta}^b(p_2) \bar{d}_{2,\gamma}^c(p_3) s_{2,\gamma}^d(p_4)$. This holds for all values of the external Dirac and color indices, and for all choices of the momenta p_i .

In a similar way, the one color-loop contractions of Q_2^{Cont} in QCD matches exactly to the PQQCD matrix element of

$$Q_{2,IA}^{\text{PQ}} = 2[\bar{s}_1^a L d_2^a][\bar{s}_2^b L d_1^b]. \quad (22)$$

Here, the subscript ‘‘ I ’’ indicates matching with a one color-loop contraction, while ‘‘ A ’’ distinguishes the operator from a similar one introduced below. Note that this operator differs from $Q_{2,II}^{\text{PQ}}$ only by the interchange $d_1 \leftrightarrow d_2$ between the bilinears, while keeping each bilinear a color singlet. In particular, no Fierz transformation

has been done on Q_2^{Cont} , so that the exact matching holds for $D = 4 - 2\epsilon$.

Repeating this exercise for Q_3^{Cont} one finds that the PQ operator corresponding to its two and one color-loop contractions are, respectively,

$$Q_{3,II}^{\text{PQ}} = 2[\bar{s}_1^a \sigma_{\mu\nu} L d_1^a][\bar{s}_2^b \sigma_{\mu\nu} L d_2^b], \quad (23)$$

$$Q_{3,IA}^{\text{PQ}} = 2[\bar{s}_1^a \sigma_{\mu\nu} L d_2^a][\bar{s}_2^b \sigma_{\mu\nu} L d_1^b]. \quad (24)$$

To write a matching equation involving operators we form the linear combinations

$$Q_{j,\pm}^{\text{PQ}} = Q_{j,II}^{\text{PQ}} \pm Q_{j,IA}^{\text{PQ}} \quad (j = 2, 3). \quad (25)$$

Our claim is that, for matrix elements involving the external operators described above, we have, to all orders in PT

$$Q_j^{\text{Cont}} \cong Q_{j,+}^{\text{PQ}} \quad (j = 2, 3). \quad (26)$$

This is our first matching equation. The two operators on the r.h.s. are needed to obtain both Wick contractions of the operator on the l.h.s. The symbol “ \cong ” indicates that this is not a true operator matching, but rather that the matrix elements *of the type described above* agree between the two theories. This is sufficient for our purposes since these are the matrix elements of interest.

The difference operators $Q_{j,-}^{\text{PQ}}$ in Eq. (25) do not play a role in the matching to Q_j^{Cont} . In fact, they are PQQCD operators with no counterparts in the $\Delta S = 2$ sector of QCD. We will use them, however, in the next stage of the calculation.

As already noted, when doing a perturbative calculation of the matrix elements described above, one encounters additional, evanescent operators which must be dealt with in order to renormalize the matrix elements. These are local operators with Dirac structures that vanish when $D = 4$. In order for the above-described exact matching to hold after renormalization, evanescent operators must be treated in the same way in both QCD and PQQCD. Doing so is, in fact, completely straightforward, since the treatment in QCD is already done contraction by contraction. Concrete examples of this statement are given in the explicit calculation of Appendix A.

We stress that, although the exact equality of matrix elements described in this subsection is almost trivial, it is nevertheless useful in order to set-up the next, non-trivial, stage of the matching. We also note that our argument is a minor adaptation of that used in Ref. [9] to show how the anomalous dimensions of $\Delta F = 1$ operators with flavor $\bar{s}d\bar{u}c$ can be related to those of $\Delta S = 2$ operators.

C. Second Step: Basis Change in PQQCD

At this stage we have succeeded in exactly converting the desired QCD calculation into one in PQQCD. The

next step is to change the operator basis in PQQCD. Essentially, we are doing a Fierz transform on the operators which match with one color-loop contractions in QCD, but taking into account the failure of Fierz transforms away from $D = 4$. This step is useful since the new basis in PQQCD matches straightforwardly onto the lattice theory.

We collect the operators discussed in the previous subsection into a vector,

$$\overrightarrow{\mathcal{O}^{\text{PQA}}} = \{Q_{2,+}^{\text{PQ}}, Q_{3,+}^{\text{PQ}}, Q_{2,-}^{\text{PQ}}, Q_{3,-}^{\text{PQ}}\}. \quad (27)$$

We will change from this basis to

$$\overrightarrow{\mathcal{O}^{\text{PQB}}} = \{Q_{2,I}^{\text{PQ}}, Q_{2,II}^{\text{PQ}}, Q_{3,I}^{\text{PQ}}, Q_{3,II}^{\text{PQ}}\}. \quad (28)$$

Here $Q_{2,II}^{\text{PQ}}$ and $Q_{3,II}^{\text{PQ}}$ are defined in Eqs. (21) and (23) above, while

$$Q_{2,I}^{\text{PQ}} \equiv \mathcal{O}_1^{\text{PQB}} = 2[\bar{s}_1^a L d_1^b][\bar{s}_2^b L d_2^a] \quad (29)$$

$$Q_{3,I}^{\text{PQ}} \equiv \mathcal{O}_3^{\text{PQB}} = 2[\bar{s}_1^a \sigma_{\mu\nu} L d_1^b][\bar{s}_2^b \sigma_{\mu\nu} L d_2^a]. \quad (30)$$

These are the two operators one obtains from $Q_{2,IA}^{\text{PQ}}$ and $Q_{3,IA}^{\text{PQ}}$ by interchanging d_2^b and d_1^b . For $D = 4$ such an interchange is brought about by a Fierz transformation, which also effects the Dirac structure. Specifically, we have

$$Q_{2,IA}^{\text{PQ}} \stackrel{D=4}{=} -\frac{1}{2}Q_{2,I}^{\text{PQ}} + \frac{1}{8}Q_{3,I}^{\text{PQ}} \quad (31)$$

$$Q_{3,IA}^{\text{PQ}} \stackrel{D=4}{=} 6Q_{2,I}^{\text{PQ}} + \frac{1}{2}Q_{3,I}^{\text{PQ}}. \quad (32)$$

so that

$$\mathcal{O}_k^{\text{PQA}} \stackrel{D=4}{=} R_{k\ell} \mathcal{O}_\ell^{\text{PQB}}, \quad (33)$$

with

$$R = \begin{pmatrix} -\frac{1}{2} & 1 & \frac{1}{8} & 0 \\ 6 & 0 & \frac{1}{2} & 1 \\ \frac{1}{2} & 1 & -\frac{1}{8} & 0 \\ -6 & 0 & -\frac{1}{2} & 1 \end{pmatrix}. \quad (34)$$

This means that tree-level matrix elements with the external fields described in the previous subsection will be related by the same linear transformation

$$\langle \mathcal{O}_k^{\text{PQA}} \rangle^{(0)} = R_{k\ell} \langle \mathcal{O}_\ell^{\text{PQB}} \rangle^{(0)}, \quad (35)$$

Here the superscript indicates the order in α .

This simple relation does not hold beyond tree level, since the Fierz transforms (32) fail for $D = 4 - 2\epsilon$. This is a standard situation in renormalization theory, explained clearly, for example, in Ref. [9]. The basis must be extended to include evanescent operators. At one-loop order, all one needs, in fact, is a set of projectors which pick out the components of the desired operators from expressions in $4 - 2\epsilon$ dimensions. The projectors for the

operators we consider have been given in Ref. [9], and are conveniently summarized in Ref. [18]. The general result is that one-loop anomalous dimensions are the same in the two bases (once the linear transformation given in Eq. (33) is taken into account), while finite parts of one-loop matrix elements (and correspondingly two-loop anomalous dimensions) can be different. This is thus an example of non-trivial operator matching, although simplified because both sets of operators are defined in the same theory.

To determine the one-loop matching between the bases one calculates the one-loop matrix elements with the same external fields and equates them. After renormalization, these matrix elements take the forms

$$\langle \mathcal{O}_k^{\text{PQA}} \rangle^{(1)} = Z_{k\ell}^{\text{PQA}} \langle \mathcal{O}_\ell^{\text{PQA}} \rangle^{(0)}, \quad (36)$$

$$Z_{k\ell}^{\text{PQA}} = \delta_{k\ell} + \frac{\alpha}{4\pi} \left[\gamma_{k\ell}^{\text{PQ}} \log(\lambda/\mu) + C_{k\ell}^{\text{PQA}} \right], \quad (37)$$

and

$$\langle \mathcal{O}_k^{\text{PQB}} \rangle^{(1)} = Z_{k\ell}^{\text{PQB}} \langle \mathcal{O}_\ell^{\text{PQB}} \rangle^{(0)}, \quad (38)$$

$$Z_{k\ell}^{\text{PQB}} = \delta_{k\ell} + \frac{\alpha}{4\pi} \left[(R^{-1} \gamma^{\text{PQ}} R)_{k\ell} \log(\lambda/\mu) + C_{k\ell}^{\text{PQB}} \right]. \quad (39)$$

Here λ is an infrared cut-off (for which we use a gluon mass), μ the renormalization scale, and γ^{PQ} the one-loop anomalous dimension in the PQA basis. The factors of R^{-1} and R in the result for Z^{PQB} are needed so that the one-loop anomalous dimensions match once the linear transformation (33) is taken into account. C^{PQA} and C^{PQB} are the finite parts of the one-loop result.

Equating $\langle \mathcal{O}_k^{\text{PQA}} \rangle^{(1)}$ with $R_{k\ell} \langle \mathcal{O}_\ell^{\text{PQB}} \rangle^{(1)}$ (a step that can be done in $D = 4$ since the matrix elements have been renormalized), and using (35), one finds our second matching equation

$$\mathcal{O}_k^{\text{PQA}} \cong \left\{ R_{k\ell} + \frac{\alpha}{4\pi} \left[(C^{\text{PQA}} R)_{k\ell} - (R C^{\text{PQB}})_{k\ell} \right] \right\} \mathcal{O}_\ell^{\text{PQB}}. \quad (40)$$

The precise meaning of this equation is that the one-loop matrix elements of the operators on the two sides agree, as long as one uses the same definitions of evanescent operators as were used to determine the matrices C^{PQA} and C^{PQB} . We still use the symbol \cong , although here the theory is the same on both sides of the matching, because we want to allow for the possibility of using a different renormalization scheme for the two bases.

We calculate the difference matrix $C^{\text{PQA}} R - R C^{\text{PQB}}$ in Appendix A. It is convenient to use different definitions of evanescent operators for the PQA and PQB bases. For the former we use the definitions of Ref. [9], so that we are ultimately matching to an operator basis in which we know the two-loop anomalous dimensions. For the PQB basis, however, we adopt the NDR' scheme, which was introduced in Ref. [10]. This is a convenient choice as it allows us to piggyback on previous one-loop calculations. We stress, however, that even if we use the definitions of Ref. [9] in both bases, the one-loop matching would be nontrivial.

D. Third Step: PQCD to Continuum Staggered Theory

The next step is to match to the theory obtained in the continuum limit of a staggered lattice theory, which we refer to as the ‘‘SPQ’’ theory (with S for staggered). This differs from PQCD by the presence of additional tastes. Specifically, this new theory has valence quarks S_j and D_j , with $j = 1, 2$, in addition to the (rooted) sea quarks. As above, upper-case letters indicate the presence of four tastes.³

The operators we consider in the SPQ theory are simple generalizations of those in the PQB basis in PQCD. They are obtained by replacing lower-case fields with their upper-case versions, and inserting the taste matrix ξ_5 . For example,

$$Q_{2,I}^{\text{PQ}} = 2[\bar{s}_1^a L d_1^b][s_2^b L d_2^a] \\ \rightarrow 2[\bar{S}_1^a (L \otimes \xi_5) D_1^b][\bar{S}_2^b (L \otimes \xi_5) D_2^a]. \quad (41)$$

In addition we will keep only the positive parity parts of the operators, since these are the parts which contribute to the $K^0 - \bar{K}^0$ matrix elements in which we are ultimately interested. This has no impact on anomalous dimensions or matching coefficients. In this way we arrive at the basis

$$\mathcal{O}_1^{\text{SPQ}} = 2 \left([\bar{S}_1^a (\mathbf{1} \otimes \xi_5) D_1^b][\bar{S}_2^b (\mathbf{1} \otimes \xi_5) D_2^a] \right. \\ \left. + [\bar{S}_1^a (\gamma_5 \otimes \xi_5) D_1^b][\bar{S}_2^b (\gamma_5 \otimes \xi_5) D_2^a] \right) \quad (42)$$

$$\mathcal{O}_2^{\text{SPQ}} = 2 \left([\bar{S}_1^a (\mathbf{1} \otimes \xi_5) D_1^a][\bar{S}_2^b (\mathbf{1} \otimes \xi_5) D_2^b] \right. \\ \left. + [\bar{S}_1^a (\gamma_5 \otimes \xi_5) D_1^a][\bar{S}_2^b (\gamma_5 \otimes \xi_5) D_2^b] \right) \quad (43)$$

$$\mathcal{O}_3^{\text{SPQ}} = 4[\bar{S}_1^a (\sigma_{\mu\nu} \otimes \xi_5) D_1^b][\bar{S}_2^b (\sigma_{\mu\nu} \otimes \xi_5) D_2^a] \quad (44)$$

$$\mathcal{O}_4^{\text{SPQ}} = 4[\bar{S}_1^a (\sigma_{\mu\nu} \otimes \xi_5) D_1^a][\bar{S}_2^b (\sigma_{\mu\nu} \otimes \xi_5) D_2^b]. \quad (45)$$

Note that for the ‘‘tensor’’ operators $\mathcal{O}_{3,4}^{\text{SPQ}}$ there is only one term, since the operators differing by a factor of $\gamma_5 \cdot \gamma_5$ are identical, and can thus be combined. This changes the overall factor from 2 to 4.

We now consider the matching between matrix elements of the PQB basis operators in PQCD and those of the above-described operators in the SPQ theory. In PQCD we use the external operators $\bar{d}_1 \gamma_5 s_1$ and $\bar{d}_2 \gamma_5 s_2$, as already discussed in Sec. III B. In the SPQ theory we use $\bar{D}_1 (\gamma_5 \otimes \xi_5) S_1$ and $\bar{D}_2 (\gamma_5 \otimes \xi_5) S_2$. Thus only positive parity operators contribute to the matrix elements. We now observe that, at any order in PT, the diagrams contributing to the matrix elements of $\mathcal{O}_k^{\text{PQB}}$ in the PQ theory are identical to those contributing to the corresponding matrix elements of $\mathcal{O}_k^{\text{SPQ}}$ in the SPQ theory, aside from the presence of the taste matrices $\xi_5 \cdot \xi_5$.

³ The SPQ theory differs from the staggered theory discussed in Sec. III A in which there was only one S and one D quark.

Given the exact taste symmetry of the SPQ theory, however, the extra taste factors lead only to an overall factor of N_T^2 , which can be removed by hand. Thus, as long as we use the analogous choices for evanescent operators in the two theories,⁴ there is an exact matching of matrix elements. We write this result as

$$\mathcal{O}_k^{\text{PQB}} \cong \mathcal{O}_k^{\text{SPQ}}, \quad (46)$$

where we are stretching the meaning of “ \cong ” here to include the provisos that taste factors are removed and only a particular class of matrix elements is considered. We also note that a consequence of this exact matching is that anomalous dimensions agree to all orders.

E. Final Step: Continuum to Lattice Staggered Theory

The final matching step is between the SPQ theory and the lattice theory using improved staggered fermions. This is a conventional matching between the same theory regularized in two different ways: dimensional regularization, with operators defined in the NDR’ scheme for the SPQ theory, and lattice regularization, for which no issues of evanescent operators arise. For the operators we use in our numerical calculation, the required one-loop matching has been done in Ref. [7]. The only subtlety is that, due to the breaking of taste symmetry by lattice regularization, the basis of lattice operators which mix with one another is much larger than that in the continuum theory. As in Ref. [7], we show here only the mixing with operators having the same taste as those in the SPQ theory, namely $\xi_5 \cdot \xi_5$. These are the operators used in present simulations. Dropping operators with other tastes leads to an error suppressed by both α and by a factor of m_π^2/m_K^2 or $m_\pi^2/(4\pi f_\pi)^2$ [14].

There are six lattice operators with taste $\xi_5 \cdot \xi_5$ that enter, and we collect these into a vector:

$$\overrightarrow{\mathcal{O}^{\text{Lat}}} = \{\mathcal{O}_{S1}^{\text{Lat}}, \mathcal{O}_{S2}^{\text{Lat}}, \mathcal{O}_{P1}^{\text{Lat}}, \mathcal{O}_{P2}^{\text{Lat}}, \mathcal{O}_{T1}^{\text{Lat}}, \mathcal{O}_{T2}^{\text{Lat}}\}. \quad (47)$$

Here we are using the notation and definitions of Ref. [7]. The subscripts indicate, first, the nature of the Dirac matrices (scalar, pseudoscalar or tensor) and, second, the color contraction (one or two color-loops). We do not repeat the details here. The difference from the basis \mathcal{O}^{SPQ} of Eqs. (42-45) is that the parts of $\mathcal{O}_{1,2}^{\text{SPQ}}$ with Dirac structures $1 \cdot 1$ and $\gamma_5 \cdot \gamma_5$ have been separated in the lattice operators. This is required because they renormalize differently.

The tree-level relationship between the bases is

$$\langle \mathcal{O}_k^{\text{SPQ}} \rangle^{(0)} = 2S_{km} \langle \mathcal{O}_m^{\text{Lat}} \rangle^{(0)}, \quad (48)$$

with S the rectangular matrix

$$S = \begin{pmatrix} 1 & 0 & 1 & 0 & 0 & 0 \\ 0 & 1 & 0 & 1 & 0 & 0 \\ 0 & 0 & 0 & 0 & 4 & 0 \\ 0 & 0 & 0 & 0 & 0 & 4 \end{pmatrix}. \quad (49)$$

The overall factor of 2 in (48) appears because the definition of the lattice operators does not include the overall factors of 2 that appear in the continuum PQ operators [see Eqs. (42) and (43)]. The factors of 4 in S relating the SPQ to lattice tensor operators arise because, first, the lattice tensor operators $\mathcal{O}_{T1}^{\text{Lat}}$ and $\mathcal{O}_{T2}^{\text{Lat}}$ are defined with the indices constrained to satisfy $\mu < \nu$, rather than being freely summed as in the continuum operators, and, second, because the continuum tensor operators come with a factor of 4 rather than 2 [see Eqs. (44) and (45)].

The one-loop matrix elements in the SPQ theory, with NDR’ regularization, are

$$\begin{aligned} \langle \mathcal{O}_k^{\text{SPQ}} \rangle^{(1)} &= Z_{k\ell}^{\text{PQB}} \langle \mathcal{O}_\ell^{\text{SPQ}} \rangle^{(0)} \\ Z_{k\ell}^{\text{PQB}} &= \delta_{k\ell} + \frac{\alpha}{4\pi} \left[(R^{-1} \gamma^{\text{PQ}} R)_{k\ell} \log(\lambda/\mu) + C_{k\ell}^{\text{PQB}} \right]. \end{aligned} \quad (50)$$

This is identical to Eq. (39) because of the exact matching between the PQB and SPQ bases, Eq. (46). The one-loop lattice matrix elements take the form

$$\langle \mathcal{O}_m^{\text{Lat}} \rangle^{(1)} = \langle \mathcal{O}_m^{\text{Lat}} \rangle^{(0)} + \frac{\alpha}{4\pi} \left[\tilde{\gamma}_{mn} \log(a\lambda) + C_{mn}^{\text{Lat}} \right] \langle \mathcal{O}_n^{\text{Lat}} \rangle^{(0)}, \quad (51)$$

with $\tilde{\gamma}$ the one-loop anomalous dimension matrix in the lattice basis. This satisfies $R^{-1} \gamma^{\text{PQ}} R S = S \tilde{\gamma}$, which is simply the statement that the projection of $\tilde{\gamma}$ onto the basis corresponding to $\mathcal{O}_k^{\text{SPQ}}$ is regularization independent. Equating one-loop matrix elements after transforming the lattice results by the matrix S leads to

$$\begin{aligned} \mathcal{O}_k^{\text{SPQ}} \cong \left\{ S_{km} + \frac{\alpha}{4\pi} \left[- (R^{-1} \gamma^{\text{PQ}} R S)_{km} \log(a\mu) \right. \right. \\ \left. \left. + (C^{\text{PQB}} S)_{km} - (S C^{\text{Lat}})_{km} \right] \right\} \mathcal{O}_m^{\text{Lat}}. \end{aligned} \quad (52)$$

Note that in this case “ \cong ” means a genuine matching between operators. Taste factors match and there are no restrictions on external fields. The only provisos are that, on the right-hand side, we have dropped lattice operators having tastes other than $\xi_5 \cdot \xi_5$ and corrections proportional to powers of the lattice spacing.

F. Final Matching Results

Combining the results (26), (40), (46) and (52) we can now match continuum operators Q_2^{Cont} and Q_3^{Cont} in the

⁴ In practice, we use the NDR’ scheme for both theories.

Dirac basis [Eqs. (3) and (4)] to lattice operators:

$$Q_j^{\text{Cont}} \cong 2z_{jm} \mathcal{O}_m^{\text{Lat}} \quad (53)$$

$$z_{jm} = P_{jk} \left\{ (RS)_{km} + \frac{\alpha}{4\pi} \left[-(\gamma^{\text{PQ}} RS)_{km} \ln(a\mu) + (C^{\text{PQA}} RS - RC^{\text{PQB}} S)_{km} + (RC^{\text{PQB}} S - RSC^{\text{Lat}})_{km} \right] \right\}, \quad (54)$$

where $j = 2, 3$, $k = 1 - 4$ and $m = 1 - 6$. Here P is a rectangular matrix projecting out the first two operators from the four-dimensional PQA basis of Eq. (27). Its only non-zero elements are $P_{21} = P_{32} = 1$ [corresponding to the exact matching of Eq. (26)]. As a matrix it looks like

$$P = \begin{pmatrix} 1 & 0 & 0 & 0 \\ 0 & 1 & 0 & 0 \end{pmatrix}. \quad (55)$$

We stress again that Eq. (53) is not a true operator matching, but rather a shorthand indicating agreement (at one-loop order, and up to known taste factors) between the positive parity parts of the appropriate kaon mixing matrix elements defined using the external operators described above.

We also note that the contribution from the matching to operators in the PQB basis cancels, as can be seen from the fact that the $RC^{\text{PQB}} S$ term appears with both signs. Cancellation is expected since this is an intermediate scheme. We find it useful, however, to break the result up as shown. This simplifies the calculation (as discussed in Appendix A), and is also useful conceptually. In particular, it is the contribution from the PQA to PQB matching, i.e. the $C^{\text{PQA}} RS - RC^{\text{PQB}} S$ term, which was not previously accounted for in Refs. [7, 10, 11]. In other words, these works effectively started with the continuum PQB basis (defining the operators using the regularization scheme of Ref. [8]) and matched from this to lattice operators.

It is useful to recast our final result into the notation used in Ref. [7]:

$$z_{jm} = b_{jm} + \frac{g^2}{(4\pi)^2} \left(-\gamma_{jm} \log(\mu a) + c_{jm} \right), \quad (56)$$

$$c_{jm} = d_{jm}^{\text{Cont}} - d_{jm}^{\text{Lat}} - C_F I_{MF} T_{jm}, \quad (57)$$

with $C_F = 4/3$. Here b_{jm} gives the linear relations between operators at tree level, while d^{Cont} and d^{Lat} are the finite parts of one-loop matrix elements in continuum and lattice regularizations, respectively. The term proportional to the matrix T appears if one mean-field improves the lattice operators, with I_{MF} the appropriate lattice integral. Details are given in Ref. [7]. This contribution is, strictly speaking, part of d^{Lat} but this separation allows one to see the numerical impact of mean-field improvement. We note that below we use the formula (57) not only for $j = 2, 3$ but also for $j = 4, 5$.

TABLE I. Components of the matching coefficients for Q_2^{Cont} , as defined in Eq. (57). The d^{Lat} are for HYP-smear'd valence fermions and operators and the Symanzik gauge action. The last column gives the numerical values for the complete one-loop matching coefficients z_{2m} for mean-field improved operators (for which $I_{MF} = 0.722795$) on the MILC ultrafine lattices ($\alpha = 0.2098$) and with $\mu a = 1$.

Operator	m	b_{2m}	γ_{2m}	d_{2m}^{Cont}	d_{2m}^{Lat}	T_{2m}	z_{2m}
$\mathcal{O}_{S1}^{\text{Lat}}$		-1/2	6	-11/6	2.335	-1	-0.554
$\mathcal{O}_{S2}^{\text{Lat}}$		1	-10	+13/6	-14.528	6	1.182
$\mathcal{O}_{P1}^{\text{Lat}}$		-1/2	6	-11/6	3.174	-1	-0.568
$\mathcal{O}_{P2}^{\text{Lat}}$		1	-10	+13/6	4.061	-2	1.001
$\mathcal{O}_{T1}^{\text{Lat}}$		1/2	-14/3	+5/6	-2.518	1	0.540
$\mathcal{O}_{T2}^{\text{Lat}}$		0	2/3	-1/2	0.012	0	-0.009

TABLE II. Components of the matching coefficients for Q_3^{Cont} . Notation as in Table I.

Operator	m	b_{3m}	γ_{3m}	d_{3m}^{Cont}	d_{3m}^{Lat}	T_{3m}	z_{3m}
$\mathcal{O}_{S1}^{\text{Lat}}$		6	88	+50/3	-13.703	12	6.314
$\mathcal{O}_{S2}^{\text{Lat}}$		0	-40	-46/3	-15.035	0	-0.005
$\mathcal{O}_{P1}^{\text{Lat}}$		6	88	+50/3	-23.769	12	6.482
$\mathcal{O}_{P2}^{\text{Lat}}$		0	-40	-46/3	15.165	0	-0.509
$\mathcal{O}_{T1}^{\text{Lat}}$		2	8/3	-14/3	-8.164	4	1.994
$\mathcal{O}_{T2}^{\text{Lat}}$		4	136/3	+6	-12.376	8	4.178

Comparing Eqs. (57) and (54), we see that

$$b_{jm} = (PRS)_{jm} \quad (58)$$

$$\gamma_{jm} = (P\gamma^{\text{PQ}} RS)_{jm} \quad (59)$$

$$d_{jm}^{\text{Cont}} = (PC^{\text{PQA}} RS)_{jm} \quad (60)$$

$$d_{jm}^{\text{Lat}} = (PRSC^{\text{Lat}})_{jm} - C_F I_{MF} T_{jm}. \quad (61)$$

The anomalous dimension matrix γ^{PQ} can be obtained, for example, from Ref. [9]. The new quantity d^{Cont} is calculated in App. A. The finite part of the lattice one-loop matrix elements, d^{Lat} , and the mean-field improvement matrix T are calculated for our choice of operators and action in Ref. [7]. We collect all these results in Tables I and II.

We include in the last column of each table the numerical values of the matching coefficients for mean-field improved operators on the finest MILC ensemble used in our companion numerical study [3, 5]. These are the operators we use in practice. Comparing the results for z_{mj} to the tree-level values, b_{mj} shows that the one-loop perturbative corrections are $\sim 5\%$.

As noted above, the matching results of Ref. [7] for the operators Q_1^{Cont} , Q_4^{Cont} and Q_5^{Cont} remain valid, because the missing PQA to PQB matching step turns out to have a vanishing one-loop coefficient. This is explained in Appendix A 5. However, since the results in Ref. [7] are presented for operators in the SUSY basis, and also for

TABLE III. Components of the matching coefficients for Q_4^{Cont} . Notation as in Table I.

Operator m	b_{4m}	γ_{4m}	d_{4m}^{Cont}	d_{4m}^{Lat}	T_{4m}	z_{4m}
$\mathcal{O}_{S1}^{\text{Lat}}$	0	0	-3	0	0	-0.050
$\mathcal{O}_{S2}^{\text{Lat}}$	1	-16	+23/3	-16.0196	6	1.299
$\mathcal{O}_{P1}^{\text{Lat}}$	0	0	+3	0	0	0.050
$\mathcal{O}_{P2}^{\text{Lat}}$	-1	16	-23/3	-5.0862	2	-1.075
$\mathcal{O}_{V1}^{\text{Lat}}$	-1/2	8	-23/6	2.7193	-1	-0.593
$\mathcal{O}_{V2}^{\text{Lat}}$	0	0	+3/2	0.3401	0	0.019
$\mathcal{O}_{A1}^{\text{Lat}}$	1/2	-8	+23/6	-2.9543	1	0.597
$\mathcal{O}_{A2}^{\text{Lat}}$	0	0	-3/2	0.3651	0	-0.031

TABLE IV. Components of the matching coefficients for Q_5^{Cont} . Notation as in Table I.

Operator m	b_{5m}	γ_{5m}	d_{5m}^{Cont}	d_{5m}^{Lat}	T_{5m}	z_{5m}
$\mathcal{O}_{S1}^{\text{Lat}}$	-2	-4	-1/3	6.835	-4	-2.055
$\mathcal{O}_{S2}^{\text{Lat}}$	0	12	1	4.892	0	-0.065
$\mathcal{O}_{P1}^{\text{Lat}}$	2	4	1/3	-10.191	4	2.111
$\mathcal{O}_{P2}^{\text{Lat}}$	0	-12	-1	5.174	0	-0.103
$\mathcal{O}_{V1}^{\text{Lat}}$	0	-6	-1/2	-0.537	0	0.001
$\mathcal{O}_{V2}^{\text{Lat}}$	1	2	1/6	-8.083	4	1.073
$\mathcal{O}_{A1}^{\text{Lat}}$	0	6	1/2	0.537	0	-0.001
$\mathcal{O}_{A2}^{\text{Lat}}$	-1	-2	-1/6	-0.179	0	-1.000

completeness, we collect the results for Q_4^{Cont} and Q_5^{Cont} in Tables III and IV. The results for the B_K operator Q_1^{Cont} can be read directly from Ref. [7].

To complete the description of the matching results used in Refs. [3, 5], we must also consider the denominator of the B -parameters defined in Eq. (8). The matching of the pseudoscalar bilinears in the denominator is given by

$$\bar{s}\gamma_5 d \cong z_P \mathcal{O}_P^{\text{Lat}} \quad (62)$$

$$\mathcal{O}_P^{\text{Lat}} = \bar{\chi}_s (\overline{\gamma_5 \otimes \xi_5}) \chi_d, \quad (63)$$

where, as above, the symbol \cong implies matching of matrix elements (here connecting the vacuum to an appropriate kaon or antikaon) up to taste factors (here a single factor of N_T since there is only one ‘‘taste loop’’). The notation for the staggered bilinear is as in Ref. [19]. For the bilinear matrix elements we do not need to introduce the extra d and s quarks of the PQQCD and SPQ theories, since there is only one contraction. For the same reason, there is no contraction factor of 2 in Eq. (62) [as compared, say, to Eq. (53)]. The one-loop result for z_P is [19]

$$z_P = 1 + \frac{\alpha}{4\pi} (8 \log(\mu a) + 10/3 - 1.57938). \quad (64)$$

This is for the continuum bilinear defined in the NDR scheme and the lattice bilinear composed of HYP-smear valence fermions with Symanzik-improved glue.

Note that the lattice operator involves no gauge links and thus cannot be mean-field improved.

In terms of lattice operators, the B -parameters thus become

$$B_i(\mu) = \frac{2 \langle \bar{K}_{P1}^0 | z_{ij} \mathcal{O}_j^{\text{Lat}} | K_{P2}^0 \rangle}{N_i \langle \bar{K}_P | z_P \mathcal{O}_P^{\text{Lat}} | 0 \rangle \langle 0 | z_P \mathcal{O}_P^{\text{Lat}} | K_0 \rangle}. \quad (65)$$

This is now an equality (up to two-loop and discretization corrections) since the taste factors cancel between numerator and denominator.

IV. RENORMALIZATION GROUP EVOLUTION

In our numerical calculations, we match matrix elements of lattice operators to those of continuum operators using Eqs. (53) and (54). To avoid large logarithms in this matching, we set $\mu = 1/a$. Before taking the continuum limit, we must evolve the resulting matrix elements to a common scale. We do this using the most accurate anomalous dimensions available, which in this case are of two-loop order. Although this is a standard procedure, there are some subtleties which arise for the operators under consideration. In this section we discuss these subtleties.

RG evolution can be expressed as

$$\langle Q_i(\mu_b) \rangle = W(\mu_b, \mu_a)_{ij} \langle Q_j(\mu_a) \rangle, \quad (66)$$

where the matrix kernel satisfies

$$\frac{d}{d \ln \mu_b} W(\mu_b, \mu_a)_{ij} = -\gamma(\mu_b)_{ij} W(\mu_b, \mu_a)_{jk}, \quad (67)$$

together with the boundary condition $W^Q(\mu_a, \mu_a)_{ij} = \delta_{ij}$. We expand the anomalous dimension matrix as

$$\gamma(\mu) = \gamma^{(0)} \frac{\alpha(\mu)}{4\pi} + \gamma^{(1)} \left(\frac{\alpha(\mu)}{4\pi} \right)^2 + \dots \quad (68)$$

Results for $\gamma^{(0)}$ and $\gamma^{(1)}$ for the operators of interest are collected in Appendix B. There is mixing within the operator pairs $\{Q_2^{\text{Cont}}, Q_3^{\text{Cont}}\}$ and $\{Q_4^{\text{Cont}}, Q_5^{\text{Cont}}\}$, while Q_1^{Cont} and the pseudoscalar density do not mix.

To evolve the B -parameters B_{2-5} , we first take out the normalization factors N_i from Eq. (8) by defining

$$R_i(\mu) \equiv N_i B_i(\mu) \quad (69)$$

$$= \frac{\langle \bar{K}_0 | Q_i^{\text{Cont}} | K_0 \rangle}{\langle \bar{K}_0 | \bar{s}\gamma_5 d | 0 \rangle \langle 0 | \bar{s}\gamma_5 d | K_0 \rangle}. \quad (70)$$

These quantities can be run to a common scale, and then divided by the N_i to return to the B -parameters. Defining $W^R(\mu_b, \mu_a)$ as the RG kernel for the R_i ,

$$R_i(\mu_b) = W^R(\mu_b, \mu_a)_{ij} R_j(\mu_a), \quad (71)$$

we have

$$W^R(\mu_b, \mu_a)_{ij} = \frac{W(\mu_b, \mu_a)_{ij}}{[W^P(\mu_b, \mu_a)]^2}, \quad (72)$$

where W^P describes the evolution of the pseudoscalar density. Combining these results we arrive at

$$B_i(\mu_b) = \sum_j W^B(\mu_b, \mu_a)_{ij} B_j(\mu_a), \quad (73)$$

$$W^B(\mu_b, \mu_a)_{ij} = \frac{1}{N_i} W^R(\mu_b, \mu_a)_{ij} N_j. \quad (74)$$

We stress that Eqs. (70-74) apply only for the BSM operators (with $i, j = 2 - 5$) and not for B_K . B_K involves a different denominator, which does not run, so its running, which is diagonal, is given by the element W_{11} of the operator evolution kernel.

We can also consider anomalous dimensions for the B -parameters themselves, defined as in Eq. (67) but with $Q \rightarrow B$. This gives

$$[\gamma_B]_{ij} = \frac{N_j}{N_i} \left([\gamma_Q]_{ij} - 2\gamma_P \delta_{ij} \right), \quad (75)$$

where again $i, j = 2 - 5$. Numerical values are given in Appendix B.

A. Solutions for the Evolution Kernel

The general solution of the RG equation (67) is

$$W(\mu_b, \mu_a) = P_\alpha \exp \left(- \int_{\alpha_a}^{\alpha_b} \frac{\gamma(\alpha)}{2\beta(\alpha)} d\alpha \right), \quad (76)$$

where P_α indicates “ α -ordering” of the matrices in the integral, $\alpha_a = \alpha(\mu_a)$, $\alpha_b = \alpha(\mu_b)$, and the β -function is defined with the normalization

$$\beta(\alpha) = \frac{1}{2} \frac{d\alpha}{d \ln \mu} = -\beta_0 \frac{\alpha^2}{4\pi} - \beta_1 \frac{\alpha^3}{(4\pi)^2} + \dots, \quad (77)$$

(so that $\beta_0 = 9$ and $\beta_1 = 64$). In the literature, a standard approximate form of the general solution Eq. (76) is used when the anomalous dimension is known to two-loop order [20]:

$$W(\mu_b, \mu_a) \approx \left[1 + \frac{\alpha_b}{4\pi} J \right]^{-1} W^{(0)}(\mu_b, \mu_a) \left[1 + \frac{\alpha_a}{4\pi} J \right], \quad (78)$$

where

$$W^{(0)}(\mu_b, \mu_a) = V^{-1} \begin{pmatrix} \alpha_b \\ \alpha_a \end{pmatrix}^{\gamma_D^{(0)}/2\beta_0} V, \quad (79)$$

$$J = \frac{\beta_1 \gamma^{(0)}}{2\beta_0^2} - V^{-1} M V, \quad (80)$$

$$M_{ij} = \frac{[V \gamma^{(1)} V^{-1}]_{ij}}{2\beta_0 + (\gamma_D^{(0)})_{jj} - (\gamma_D^{(0)})_{ii}}. \quad (81)$$

Here V is the matrix that diagonalizes $\gamma^{(0)}$,

$$V \gamma^{(0)} V^{-1} = \gamma_D^{(0)}, \quad (82)$$

and

$$\left[\begin{pmatrix} \alpha_b \\ \alpha_a \end{pmatrix}^{\gamma_D^{(0)}/2\beta_0} \right]_{ij} = \delta_{ij} \begin{pmatrix} \alpha_b \\ \alpha_a \end{pmatrix}^{(\gamma_D^{(0)})_{ii}/2\beta_0}. \quad (83)$$

In practice, we use an alternative form of Eq. (78),

$$W(\mu_b, \mu_a) \approx W^{(0)}(\mu_b, \mu_a) + \frac{1}{4\pi} \left[\alpha_a W^{(0)}(\mu_b, \mu_a) J - \alpha_b J W^{(0)}(\mu_b, \mu_a) \right] \quad (84)$$

$$\equiv W^{(0)}(\mu_b, \mu_a) + \frac{1}{4\pi} V^{-1} A V. \quad (85)$$

This form is equivalent at the order we work, and is more convenient for the following discussion.

This approximate analytic solution fails, however, if, for some choice of $i \neq j$,

$$2\beta_0 + (\gamma_D^{(0)})_{jj} - (\gamma_D^{(0)})_{ii} = 0, \quad (86)$$

for then M diverges [see Eq. (81)]. This indeed happens for the pair of operators $Q_{4,5}^{\text{Cont}}$, since the eigenvalues of $\gamma^{(0)}$ differ by exactly $2\beta_0 = 18$ (see Appendix B). We stress that this is a failure of the approximation method, and does not indicate a breakdown in perturbative convergence for W itself. Indeed, the truncated version of the differential equation (67) is not singular.

The problem can be resolved using the analytic continuation technique introduced in Ref. [12]. The outcome is that, for each $\{i, j\}$ pair for which the denominator of M_{ij} vanishes [i.e. for which Eq. (86) holds], the element A_{ij} of the matrix A in Eq. (85) is replaced by

$$\frac{[V \gamma^{(1)} V^{-1}]_{ij}}{2\beta_0} \alpha_b \ln \left(\frac{\alpha_b}{\alpha_a} \right) \begin{pmatrix} \alpha_b \\ \alpha_a \end{pmatrix}^{(\gamma_D^{(0)})_{jj}/2\beta_0}. \quad (87)$$

The derivation of this result is given in Ref. [12].

We have checked these analytic expressions by solving the RG equation (67) numerically, after truncating the anomalous dimension and β -function. Specifically, we use the variable $t = (\ln \alpha)/(2\beta_0)$ which satisfies, at two-loop order,

$$\frac{dt}{d \ln \mu} = -\frac{\alpha}{4\pi} \left(1 + \frac{\beta_1}{\beta_0} \frac{\alpha}{4\pi} \right), \quad (88)$$

Then

$$\frac{dW(t_b, t_a)}{dt_b} = \left(\frac{dt_b}{d \ln \mu_b} \right)^{-1} \frac{dW(\mu_b, \mu_a)}{d \ln \mu_b} \quad (89)$$

$$\approx \frac{\gamma^{(0)} + \frac{\alpha_b}{4\pi} \gamma^{(1)}}{1 + \frac{\alpha_b}{4\pi} \frac{\beta_1}{\beta_0}} W(t_b, t_a) \quad (90)$$

$$\approx \left(\gamma^{(0)} + \frac{\alpha_b}{4\pi} \left[\gamma^{(1)} - \frac{\beta_1}{\beta_0} \gamma^{(0)} \right] \right) W(t_b, t_a), \quad (91)$$

where the approximations are allowed since they involve dropping terms of the same order as the missing three-loop contributions. The resulting equation is straightforward to integrate numerically.

We find that, for the ranges over which we evolve, the analytic and numerical results for the elements of W agree to ~ 0.01 or better. For example, the evolution matrix for the operators in the full Dirac basis from $\mu_a = 3 \text{ GeV}$ to $\mu_b = 2 \text{ GeV}$ is

$$W_{\text{anal}} = \begin{pmatrix} 1.0349 & 0 & 0 & 0 & 0 \\ 0 & 0.8862 & 0.0013 & 0 & 0 \\ 0 & -0.4786 & 1.1532 & 0 & 0 \\ 0 & 0 & 0 & 0.8289 & 0.0106 \\ 0 & 0 & 0 & 0.1310 & 1.0225 \end{pmatrix}, \quad (92)$$

using the analytic results, and

$$W_{\text{num}} = \begin{pmatrix} 1.0350 & 0 & 0 & 0 & 0 \\ 0 & 0.8863 & 0.0013 & 0 & 0 \\ 0 & -0.4789 & 1.1536 & 0 & 0 \\ 0 & 0 & 0 & 0.8291 & 0.0105 \\ 0 & 0 & 0 & 0.1308 & 1.0225 \end{pmatrix} \quad (93)$$

from the numerical solution. Here we use $\alpha(2 \text{ GeV}) = 0.2959$ and $\alpha(3 \text{ GeV}) = 0.2448$.⁵ The running between these two values is done using the four-loop β -function with $N_f = 3$. We use three active flavors (despite being in the regime where the charm is active) because this is the number of dynamical flavors in our simulations. We use the four-loop β -function (despite evolving the operators using two-loop expressions) since this incorporates some of the known higher-order terms. Numerically this is not, however, very important. For example, if we start from $\alpha(2 \text{ GeV}) = 0.2959$ and run using the two-loop β -function we find $\alpha(3 \text{ GeV}) = 0.2470$, which leads to

$$W_{2\text{-loop } \alpha} = \begin{pmatrix} 1.0333 & 0 & 0 & 0 & 0 \\ 0 & 0.8913 & 0.0012 & 0 & 0 \\ 0 & -0.4563 & 1.1460 & 0 & 0 \\ 0 & 0 & 0 & 0.8363 & 0.0101 \\ 0 & 0 & 0 & 0.1252 & 1.0214 \end{pmatrix}. \quad (94)$$

Here we have used the numerical solution of the evolution equation. We see that the elements differ by ~ 0.02 or less from those given above using four-loop running of α .

It is also interesting to see how quickly perturbation theory is converging. This is illustrated by comparing the matrices above to the one-loop result

$$W_{1\text{-loop}} = \begin{pmatrix} 1.043 & 0 & 0 & 0 & 0 \\ 0 & 0.900 & 0.0018 & 0 & 0 \\ 0 & -0.425 & 1.126 & 0 & 0 \\ 0 & 0 & 0 & 0.845 & 0 \\ 0 & 0 & 0 & 0.118 & 1.021 \end{pmatrix} \quad (95)$$

(obtained using the four-loop values of α).

As a check on our calculation of W , we can compare to the result for $W(3 \text{ GeV}, 2 \text{ GeV})$ given in Ref. [22]:⁶

$$W_{\text{MV}} = \begin{pmatrix} 1.035 & 0 & 0 & 0 & 0 \\ 0 & 0.887 & 0.001 & 0 & 0 \\ 0 & -0.474 & 1.152 & 0 & 0 \\ 0 & 0 & 0 & 0.830 & 0.011 \\ 0 & 0 & 0 & 0.130 & 1.022 \end{pmatrix} \quad (96)$$

This agrees with our results to better than the ± 0.02 variation between approximation methods, thus checking our transcription of anomalous dimensions and calculation of evolution matrices.

Results for the evolution kernels needed in our numerical calculations are collected in Appendix C.

B. Running of “golden” combinations

The quantities

$$B_{23} \equiv \frac{B_2}{B_3}, \quad B_{45} \equiv \frac{B_4}{B_5}, \quad B_{24} \equiv B_2 \times B_4 \quad \text{and} \quad B_{21} = \frac{B_2}{B_K} \quad (97)$$

were found in Ref. [14] to have no one-loop chiral logarithms in SU(2) chiral perturbation theory. Thus they are expected to have better controlled chiral extrapolations than the B -parameters themselves. Following Ref. [13], we refer to them as “golden” combinations.

We are using these quantities in our companion lattice calculations [3, 5]. Indeed our central values for the B_j are reconstructed from these four golden quantities and our result for B_K . Thus it is useful to have the RG running formulae directly for the golden combinations. The evolution of the B -parameters is given by Eq. (73), with the evolution kernel W^B being non-vanishing only within the (1), (2, 3), and (4, 5) blocks. From this we can

⁵ These values are obtained at $N_f = 3$ by following the four-loop running procedure given in Ref. [21] starting from $\alpha(M_Z) = 0.118$ with $M_Z = 91187.6 \text{ MeV}$.

⁶ Note that Ref. [22] uses a different ordering of operators and also quotes the transpose of W . Here we have converted to our notation.

determine the evolution of the golden combinations:

$$B_{23}(\mu_b) = \frac{W^B(\mu_b, \mu_a)_{22}B_{23}(\mu_a) + W^B(\mu_b, \mu_a)_{23}}{W^B(\mu_b, \mu_a)_{32}B_{23}(\mu_a) + W^B(\mu_b, \mu_a)_{33}}, \quad (98)$$

$$B_{45}(\mu_b) = \frac{W^B(\mu_b, \mu_a)_{44}B_{45}(\mu_a) + W^B(\mu_b, \mu_a)_{45}}{W^B(\mu_b, \mu_a)_{54}B_{45}(\mu_a) + W^B(\mu_b, \mu_a)_{55}}, \quad (99)$$

$$\begin{aligned} B_{24}(\mu_b) &= B_{24}(\mu_a) \\ &\times \left(W^B(\mu_b, \mu_a)_{22} + W^B(\mu_b, \mu_a)_{23}/B_{23}(\mu_a) \right) \\ &\times \left(W^B(\mu_b, \mu_a)_{44} + W^B(\mu_b, \mu_a)_{45}/B_{45}(\mu_a) \right), \end{aligned} \quad (100)$$

$$\begin{aligned} B_{21}(\mu_b) &= B_{21}(\mu_a) \\ &\times \frac{W^B(\mu_b, \mu_a)_{22} + W^B(\mu_b, \mu_a)/B_{23}(\mu_a)}{W(\mu_b, \mu_a)_{11}}. \end{aligned} \quad (101)$$

Note that the running of B_{23} depends only on the initial value of this quantity, which is the case also for B_{45} . For B_{24} , however, one needs the initial values of B_{24} , B_{23} and B_{45} , while for B_{21} one needs the initial values of both B_{21} and B_{23} . Note also that the denominator of Eq. (101) involves W rather than W^B , because the denominator of B_K involves axial currents which have vanishing anomalous dimensions.

ACKNOWLEDGMENTS

The research of W. Lee is supported by the Creative Research Initiatives Program (2013-003454) of the NRF grant funded by the Korean government (MSIP). W. Lee would like to acknowledge the support from KISTI supercomputing center through the strategic support program for the supercomputing application research [No. KSC-2013-G3-01]. The work of S. Sharpe is supported in part by the US DOE grant no. DE-FG02-96ER40956.

Appendix A: Calculation of Finite Parts of Matching Matrices

In this section we describe the calculation of the finite part of the continuum contribution to the one-loop matrix elements of the operators Q_j^{Cont} [Eqs. (3-6)]. The main focus is on Q_2^{Cont} and Q_3^{Cont} . Specifically, we determine C^{PQA} , which is needed to determine d^{Cont} in Eq. (60). The calculation turns out to be simplified by first calculating the difference $C^{\text{PQA}}R - RC^{\text{PQB}}$, which arises in the matching step described in Sec. III C, and then determining C^{PQB} . Combining these two results we obtain C^{PQA} .

As explained in the main text, the required matching calculation involves a change of operator basis *and*

NDR scheme in the PQCD continuum theory. Since the change of basis is, for $D = 4$, accomplished by a Fierz transformation described by the matrix R , any contribution to the one-loop matrix elements in Eqs. (37) and (39) whose calculation is consistent with the Fierz transformation will cancel in the difference $C^{\text{PQA}}R - RC^{\text{PQB}}$. This is, for example, why there is no anomalous dimension term in Eq.(40). It also means that wave function renormalization diagrams do not contribute. The upshot is that we need only keep those parts of the one-loop diagrams which containing $O(\epsilon)$ contributions *arising from the projections onto the basis operators used in the two NDR schemes* (or, equivalently, from the subtraction of evanescent operators). These will multiply the $1/\epsilon$ pole from the loop integral, leading to finite contributions to the matrix elements. All other parts of the calculation are common to the two schemes and cancel in the difference.

We call the projection-related finite contributions $C^{\text{PQA,proj}}$ and $C^{\text{PQB,proj}}$. We stress that they are not the complete finite contributions, so that, e.g., $C^{\text{PQA,proj}} \neq C^{\text{PQA}}$. But they are the only parts we need in order to calculate the difference $C^{\text{PQA}}R - RC^{\text{PQB}}$.

With this background in place, we now explain, in turn, the calculation of $C^{\text{PQA,proj}}$, $C^{\text{PQB,proj}}$ and C^{PQB} , from which we obtain C^{PQA} . We then explain why the results for operators Q_1^{Cont} , Q_4^{Cont} and Q_5^{Cont} from Ref. [7] are not impacted by the considerations of this appendix.

1. Projection parts in PQA basis

For the PQA calculation, it is simplest to make a small further change in the basis from our canonical PQA basis (which we repeat for convenience)

$$\overrightarrow{\mathcal{O}^{\text{PQA}}} = \{Q_{2,+}^{\text{PQ}}, Q_{3,+}^{\text{PQ}}, Q_{2,-}^{\text{PQ}}, Q_{3,-}^{\text{PQ}}\}, \quad (A1)$$

to

$$\overrightarrow{\mathcal{O}^{\text{PQ}}} = \{Q_{2,IA}^{\text{PQ}}, Q_{2,II}^{\text{PQ}}, Q_{3,IA}^{\text{PQ}}, Q_{3,II}^{\text{PQ}}\}, \quad (A2)$$

where we recall that

$$Q_{j,\pm}^{\text{PQ}} = Q_{j,II}^{\text{PQ}} \pm Q_{j,IA}^{\text{PQ}} \quad (j = 2, 3). \quad (A3)$$

We use the same definition of evanescent operators in the PQ and PQA bases, so the two bases are exactly related by a linear transformation, namely

$$\mathcal{O}_k^{\text{PQA}} = V_{k\ell} \mathcal{O}_\ell^{\text{PQ}}, \quad (A4)$$

with

$$V = \begin{pmatrix} 1 & 1 & 0 & 0 \\ 0 & 0 & 1 & 1 \\ -1 & 1 & 0 & 0 \\ 0 & 0 & -1 & 1 \end{pmatrix}. \quad (A5)$$

Thus if we calculate C^{PQ} from

$$\begin{aligned} \langle \mathcal{O}_k^{\text{PQ}} \rangle^{(1)} &= \langle \mathcal{O}_k^{\text{PQ}} \rangle^{(0)} \\ &+ \frac{\alpha}{4\pi} \left[\gamma_{k\ell}^{\text{PQ}} \log(\lambda/\mu) + C_{k\ell}^{\text{PQ}} \right] \langle \mathcal{O}_\ell^{\text{PQ}} \rangle^{(0)}, \end{aligned} \quad (\text{A6})$$

then

$$C^{\text{PQA}} = V C^{\text{PQ}} V^{-1}. \quad (\text{A7})$$

and

$$C^{\text{PQA,proj}} = V C^{\text{PQ,proj}} V^{-1}, \quad (\text{A8})$$

where $C^{\text{PQ,proj}}$ is the finite part of the matrix element in the PQ basis arising from projections.

We now sketch the calculation of $C^{\text{PQ,proj}}$. We illustrate the method by working in detail through the example of matching for $\mathcal{O}_1^{\text{PQ}} = Q_{2,IA}^{\text{PQ}} = 2[\bar{s}_1^a L d_2^a][\bar{s}_2^b L d_1^b]$. We use the terminology that the ‘‘Dirac structure’’ of this operator is $L \cdot L$.

There are three types of one-loop diagrams, shown in Fig. 1. The Xa diagrams are those in which the gluon connects external quark and antiquark propagators which are attached to the *same* bilinear. The flavor of the bilinears depends on the operator under consideration. For $Q_{2,IA}^{\text{PQ}}$ and $Q_{3,IA}^{\text{PQ}}$ [Eq. (24)], the bilinears have flavors $\bar{s}_1 d_2$ and $\bar{s}_2 d_1$, while for $Q_{2,II}^{\text{PQ}}$ and $Q_{3,II}^{\text{PQ}}$ [defined in Eqs. (21) and (23)] they have flavors $\bar{s}_1 d_1$ and $\bar{s}_2 d_2$. For $Q_{2,IA}^{\text{PQ}}$, Xa diagrams have Dirac structure

$$\gamma_\alpha \gamma_\beta L \gamma_\beta \gamma_\alpha \cdot L = 16(1 - \epsilon) L \cdot L, \quad (\text{A9})$$

where the γ_α 's come from vertices of the Feynman gauge gluon propagator, while the γ_β 's arise from the fermion propagators after loop integration has contracted their indices. The right-hand side of (A9) is the result after performing D -dimensional Dirac algebra. In this case, the resulting operator has the same Dirac structure as the original operator for all D , so no projection is required. The loop integral gives rise to a $1/\epsilon$ pole, and the desired finite part is obtained from combining this with the factor of ϵ multiplying the operator. Taking into account the loop integral, and the fact that there are two Xa diagrams, each giving an identical contribution, one finds the rule that the desired finite part is obtained by multiplying the ϵ term in the Dirac structure by $1/(2\epsilon)$ (leading to $-16\epsilon/(2\epsilon) = -8$), as well as by the color factor. In the present case, the gluon loop simply gives back the original color structure with an overall factor of $C_F = 4/3$. In total, then, the Xa diagrams give a contribution of $-32/3$ to the diagonal element C_{11}^{PQ} .

In the Xb diagrams the gluon connects a quark attached to one bilinear to the antiquark attached to the other. Thus, for $Q_{2,IA}^{\text{PQ}}$, the Dirac structure is

$$\Gamma_b^{\text{PQ}} = \gamma_\alpha \gamma_\beta L \cdot L \gamma_\beta \gamma_\alpha. \quad (\text{A10})$$

In four dimensions one can use Fierz transformations to manipulate this structure into a linear combination of

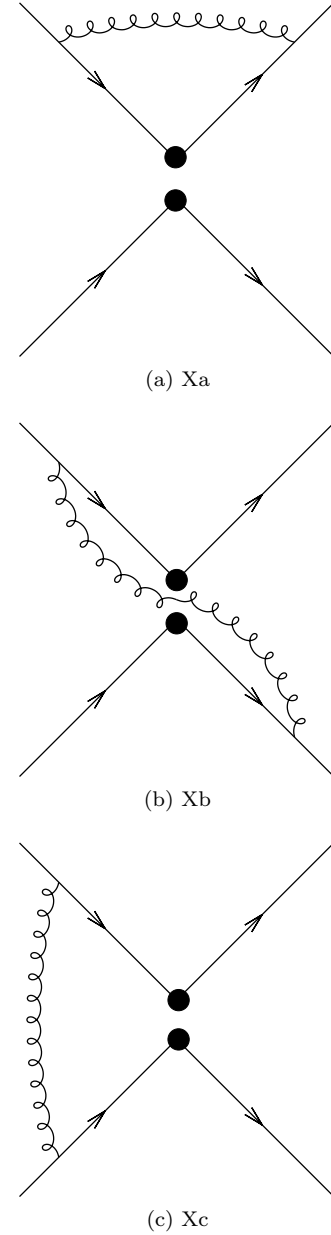


FIG. 1. Classes of one-loop diagrams, with labeling as in Ref. [23]. Each filled circle represents one of the two bilinears composing the four-fermion operator. For each diagram shown, there is a second one (not shown) in which the gluon connects the other two fermion propagators.

$L \cdot L$ and $\sigma L \cdot \sigma L$ (the latter being a shorthand for the Dirac structure of Q_3^{Cont}). For $D \neq 4$ such manipulations introduce additional operators. The contribution of these evanescent operators, which multiplies the $1/\epsilon$ pole, is then subtracted by counterterms. What remains after this subtraction depends on the choice of evanescent operators. This choice of scheme can be encapsulated into rules for projecting Dirac structures such as Γ_b^{PQ} onto the operators in the PQ basis. We use the rules for the scheme of Ref. [9], which are conveniently collected

in Appendix B of Ref. [18]. In the present example, we need Eq. (45c) from the latter work, according to which one makes the replacement

$$\Gamma_b^{\text{PQ}} \longrightarrow (4 - 2\epsilon)L \cdot L - \sigma L \cdot \sigma L. \quad (\text{A11})$$

The desired finite part is thus

$$\frac{-2\epsilon L \cdot L}{2\epsilon} = -L \cdot L, \quad (\text{A12})$$

multiplied by the color factor. The color factor is simple to work out but will not be needed.

Finally, we turn to the Xc diagrams, in which the gluon connects a quark to a quark or an antiquark to an antiquark. Here the Dirac structure is

$$\Gamma_c^{\text{PQ}} = \gamma_\alpha \gamma_\beta L \cdot \gamma_\alpha \gamma_\beta L \longrightarrow (4 - 2\epsilon)L \cdot L + \sigma L \cdot \sigma L, \quad (\text{A13})$$

where in the second step we have used the projection of Eq. (45b) of Ref. [18]. The Xc diagrams come with an additional minus sign, so the desired finite part is obtained by multiplying the ϵ term in Eq. (A13) by $-1/(2\epsilon)$. The result is

$$\frac{-2\epsilon L \cdot L}{-2\epsilon} = +L \cdot L, \quad (\text{A14})$$

multiplied by the *same* color factor as for the Xb diagrams. Thus the contributions from the Xb and Xc diagrams cancel.

The overall result is that we know the first row of $C^{\text{PQ,proj}}$,

$$C_{1k}^{\text{PQ,proj}} = (-32/3 \ 0 \ 0 \ 0). \quad (\text{A15})$$

The calculation for the operator $\mathcal{O}_2^{\text{PQ}} = Q_{2,II}^{\text{PQ}} = 2[\bar{s}_1^a L d_1^a][\bar{s}_2^b L d_2^b]$ is identical. This is because the regularization is defined relative to the contractions of external fields to the bilinears in the operator at hand, irrespective of its particular flavor structure. Since the Dirac and color structure of $Q_{2,II}^{\text{PQ}}$ are the same as that of $Q_{2,IA}^{\text{PQ}}$, the results for the two operators are in one-to-one correspondence. The only change is that d_1 and d_2 are interchanged. The upshot is that the only non-zero entry is $C_{22}^{\text{PQ,proj}} = -32/3$, so the second row of $C^{\text{PQ,proj}}$ is

$$C_{2k}^{\text{PQ,proj}} = (0 \ -32/3 \ 0 \ 0). \quad (\text{A16})$$

We now turn to the tensor operator $\mathcal{O}_3^{\text{PQ}} = Q_{3,IA}^{\text{PQ}} = 2[\bar{s}_1^a \sigma L d_2^a][\bar{s}_2^b \sigma L d_1^b]$. Here we are keeping the indices on $\sigma_{\mu\nu}$ implicit. The Xa diagrams lead to

$$\gamma_\alpha \gamma_\beta \sigma L \gamma_\beta \gamma_\alpha \cdot \sigma L \quad (\text{A17})$$

which vanishes through $O(\epsilon)$. Thus there is no finite contribution from these diagrams. For the Xb and Xc diagrams we need [using Eqs. (46c) and (46b) of Ref. [18], respectively]

$$\gamma_\alpha \gamma_\beta \sigma L \cdot \sigma L \gamma_\beta \gamma_\alpha \longrightarrow (-48 + 80\epsilon)L \cdot L + (12 - 14\epsilon)\sigma L \cdot \sigma L \quad (\text{A18})$$

and

$$\gamma_\alpha \gamma_\beta \sigma L \cdot \gamma_\alpha \gamma_\beta \sigma L \longrightarrow (48 - 80\epsilon)L \cdot L + (12 - 6\epsilon)\sigma L \cdot \sigma L. \quad (\text{A19})$$

Both types of diagram come with the same color factor, and so can be combined. The total finite part is thus (remembering the relative minus sign for the Xc diagrams)

$$80L \cdot L - 4\sigma L \cdot \sigma L. \quad (\text{A20})$$

The diagonal color factor is $-1/6$, leading to the results $C_{31}^{\text{PQ,proj}} = -80/6$ and $C_{33}^{\text{PQ,proj}} = 4/6$.

There is also an off-diagonal color factor of $1/2$. This gives rise to the combination

$$40 \times 2[\bar{s}_1^a L d_2^b][\bar{s}_2^b L d_1^a] - 2 \times 2[\bar{s}_1^a \sigma L d_2^b][\bar{s}_2^b \sigma L d_1^a]. \quad (\text{A21})$$

Neither of these two operators is in the PQ basis (nor, for that matter, in either of the PQA or PQB bases). To express this combination in the PQ basis one must do a Fierz transform, which now can be done setting $D = 4$ since the matrix elements have been renormalized:⁷

$$2[\bar{s}_1^a L d_2^b][\bar{s}_2^b L d_1^a] \stackrel{D=4}{=} -\frac{1}{2}Q_{2,II}^{\text{PQ}} + \frac{1}{8}Q_{3,II}^{\text{PQ}} \quad (\text{A22})$$

$$2[\bar{s}_1^a \sigma L d_2^b][\bar{s}_2^b \sigma L d_1^a] \stackrel{D=4}{=} 6Q_{2,II}^{\text{PQ}} + \frac{1}{2}Q_{3,II}^{\text{PQ}}. \quad (\text{A23})$$

Thus the combination in (A21) becomes

$$-32Q_{2,II}^{\text{PQ}} + 4Q_{3,II}^{\text{PQ}}. \quad (\text{A24})$$

Combining the above we find the third row of $C^{\text{PQ,proj}}$ to be

$$C_{3k}^{\text{PQ,proj}} = (-40/3 \ -32 \ 2/3 \ 4). \quad (\text{A25})$$

The calculation for the fourth row is identical to the third aside from interchanging the roles of the two contractions, and leads to

$$C_{4k}^{\text{PQ,proj}} = (-32 \ -40/3 \ 4 \ 2/3). \quad (\text{A26})$$

We can now change to the PQA basis, and find

$$C^{\text{PQA,proj}} = V C^{\text{PQ,proj}} V^{-1} = \frac{1}{3} \begin{pmatrix} -32 & 0 & 0 & 0 \\ -136 & 14 & 0 & 0 \\ 0 & 0 & -32 & 0 \\ 0 & 0 & 56 & -10 \end{pmatrix}. \quad (\text{A27})$$

In fact, we need only the first two rows, but display the full matrix for completeness and to allow checking.

⁷ At $\mathcal{O}(\epsilon)$, this Fierz transformation introduces further evanescent operators (which are included in the list in Appendix A of Ref. [9]). These must be kept in the calculation of two-loop anomalous dimensions.

2. Projection parts in PQB basis

We recall that we use the NDR' scheme of Ref. [10] in the PQB basis. In this scheme, one uses, by definition, $D = 4$ Fierz transforms to bring Xb and Xc diagrams into the form of bilinear corrections. For the Xc diagrams one also needs to charge conjugate one of the bilinears. This procedure allows one to separate the Dirac and color parts of the calculation. We note that this scheme is defined only at one-loop order, but this is not a problem, both because we are working at one-loop, and, more importantly, because we are using this scheme only as an intermediate calculational device.

We recall that the operators in the PQB basis are

$$\mathcal{O}_1^{\text{PQB}} = Q_{2,I}^{\text{PQ}} = 2[\bar{s}_1^a L d_1^b][\bar{s}_2^b L d_2^a], \quad (\text{A28})$$

$$\mathcal{O}_2^{\text{PQB}} = Q_{2,II}^{\text{PQ}} = 2[\bar{s}_1^a L d_1^a][\bar{s}_2^b L d_2^b], \quad (\text{A29})$$

$$\mathcal{O}_3^{\text{PQB}} = Q_{3,I}^{\text{PQ}} = 2[\bar{s}_1^a \sigma_{\mu\nu} L d_1^b][\bar{s}_2^b \sigma_{\mu\nu} L d_2^a], \quad (\text{A30})$$

$$\mathcal{O}_4^{\text{PQB}} = Q_{3,II}^{\text{PQ}} = 2[\bar{s}_1^a \sigma_{\mu\nu} L d_1^a][\bar{s}_2^b \sigma_{\mu\nu} L d_2^b]. \quad (\text{A31})$$

The Dirac structure of these four operators are the same as those in the PQA basis. The differences between bases are in the flavor indices (which has no impact since projections are defined relative to type of contractions) and in the color indices (which does impact the color factors).

The Xa diagrams give exactly the same finite contributions as in the PQ basis, i.e., a factor of -8 for $L \cdot L$ and 0 for $\sigma L \cdot \sigma L$.

For the Xb diagrams one must Fierz transform, calculate the finite part, and then Fierz transform back. This proceeds as follows

$$\begin{aligned} L \cdot L &\xrightarrow{\text{Fierz}} -\frac{1}{2}L \cdot L + \frac{1}{8}\sigma L \cdot \sigma L \\ &\xrightarrow{1\text{-loop}} 4L \cdot L \xrightarrow{\text{Fierz}} -2L \cdot L + \frac{1}{2}\sigma L \cdot \sigma L \end{aligned} \quad (\text{A32})$$

and

$$\begin{aligned} \sigma L \cdot \sigma L &\xrightarrow{\text{Fierz}} 6L \cdot L + \frac{1}{2}\sigma L \cdot \sigma L \\ &\xrightarrow{1\text{-loop}} -48L \cdot L \xrightarrow{\text{Fierz}} 24L \cdot L - 6\sigma L \cdot \sigma L. \end{aligned} \quad (\text{A33})$$

For the Xc diagrams there are charge conjugation steps at the beginning at end, which flip the sign of $\sigma L \cdot \sigma L$ while leaving $L \cdot L$ unchanged. Taking this into account, and including the extra sign from the Xc loop, one finds

$$L \cdot L \xrightarrow{\text{Xc}} 2L \cdot L + \frac{1}{2}\sigma L \cdot \sigma L \quad (\text{A34})$$

$$\sigma L \cdot \sigma L \xrightarrow{\text{Xc}} 24L \cdot L + 6\sigma L \cdot \sigma L. \quad (\text{A35})$$

Combining these results with the color factors, we find

$$\begin{aligned} C^{\text{PQB,proj}} &= \begin{pmatrix} -8 & 0 \\ 0 & 0 \end{pmatrix} \otimes \begin{pmatrix} -1/6 & 1/2 \\ 0 & 4/3 \end{pmatrix} \\ &+ \begin{pmatrix} -2 & 1/2 \\ 24 & -6 \end{pmatrix} \otimes \begin{pmatrix} 4/3 & 0 \\ 1/2 & -1/6 \end{pmatrix} \\ &+ \begin{pmatrix} 2 & 1/2 \\ 24 & 6 \end{pmatrix} \otimes \begin{pmatrix} -1/6 & 1/2 \\ 1/2 & -1/6 \end{pmatrix}, \\ &= \begin{pmatrix} -5/3 & -3 & 7/12 & 1/4 \\ 0 & -32/3 & 1/2 & -1/6 \\ 28 & 12 & -9 & 3 \\ 24 & -8 & 0 & 0 \end{pmatrix}. \end{aligned} \quad (\text{A36})$$

In the tensor products the first matrix acts on the Q_2, Q_3 indices while the second matrix acts on the I, II indices.

Combining this result with (A27), we find

$$C^{\text{PQA}} - RC^{\text{PQB}}R^{-1} = C^{\text{PQA,proj}} - RC^{\text{PQB,proj}}R^{-1} \quad (\text{A37})$$

$$= \begin{pmatrix} -3 & -1/12 & 0 & 0 \\ -76/3 & 5/3 & 0 & 0 \\ 0 & 0 & 3 & 5/12 \\ 0 & 0 & 44/3 & -1/3 \end{pmatrix}. \quad (\text{A38})$$

3. Finite part in PQB basis.

The final ingredient we need is the full finite part for the PQB-basis operators in the NDR' scheme. The calculation proceeds essentially as in the previous subsection, except that now we use the full finite parts for bilinears in the NDR scheme, which can be taken, e.g., from Ref. [23]. The method is explained in more detail in Ref. [8]. The result is

$$\begin{aligned} C^{\text{PQB}} &= \begin{pmatrix} 2c_S & 0 \\ 0 & 2c_T \end{pmatrix} \otimes \begin{pmatrix} -1/6 & 1/2 \\ 0 & 4/3 \end{pmatrix} \\ &+ \begin{pmatrix} (c_S+3c_T)/2 & (c_T-c_S)/8 \\ 6(c_T-c_S) & (3c_S+c_T)/2 \end{pmatrix} \otimes \begin{pmatrix} 4/3 & 0 \\ 1/2 & -1/6 \end{pmatrix} \\ &+ \begin{pmatrix} -(c_S+3c_T)/2 & (c_T-c_S)/8 \\ 6(c_T-c_S) & -(3c_S+c_T)/2 \end{pmatrix} \otimes \begin{pmatrix} -1/6 & 1/2 \\ 1/2 & -1/6 \end{pmatrix}, \end{aligned} \quad (\text{A39})$$

with $c_S = 2.5$ and $c_T = 0.5$. Numerically, the result takes its simplest form after a similarity transform with R :

$$RC^{\text{PQB}}R^{-1} = \begin{pmatrix} 31/6 & -1/24 & 0 & 0 \\ 10 & -1/6 & 0 & 0 \\ 0 & 0 & 49/6 & 5/24 \\ 0 & 0 & -2 & 17/6 \end{pmatrix}. \quad (\text{A40})$$

4. Final result for C^{PQA}

Combining Eqs. (A38) and (A40) we find

$$C^{\text{PQA}} = \begin{pmatrix} 13/6 & -1/8 & 0 & 0 \\ -46/3 & 3/2 & 0 & 0 \\ 0 & 0 & 67/6 & 5/8 \\ 0 & 0 & 38/3 & 5/2 \end{pmatrix}. \quad (\text{A41})$$

Multiplying from the right by RS leads to the results quoted in Tables I and II.

5. Other Operators

We have claimed above that the results given in Ref. [7] for the matching of operators $Q_{1,4,5}^{\text{Cont}}$ are correct, although the matching was not done completely correctly. Here we substantiate this claim.

We begin by discussing the B_K operator, Q_1^{Cont} [see Eq. (2)], for which the analysis is simplest. First we match this operator into PQQCD, as in Sec. IIIB in the main text. There is an exact matching of matrix elements with those of

$$Q_1^{\text{PQA}} = Q_{1,II}^{\text{PQ}} + Q_{1,IA}^{\text{PQ}} \quad (\text{A42})$$

$$Q_{1,II}^{\text{PQ}} = 2[\bar{s}_1^a \gamma_\mu L d_1^a][\bar{s}_2^b \gamma_\mu L d_2^b] \quad (\text{A43})$$

$$Q_{1,IA}^{\text{PQ}} = 2[\bar{s}_1^a \gamma_\mu L d_2^a][\bar{s}_2^b \gamma_\mu L d_1^b]. \quad (\text{A44})$$

This forms the one-dimensional PQA basis in this case. In Refs. [7, 10, 11] it was implicitly assumed that matrix elements of this operator are equal at one-loop order to those of following operator in the PQB basis

$$Q_1^{\text{PQB}} = Q_{1,II}^{\text{PQ}} + 2[\bar{s}_1^a \gamma_\mu L d_1^b][\bar{s}_2^b \gamma_\mu L d_2^a], \quad (\text{A45})$$

as long as one uses the *same* NDR scheme for both operators. In other words, it was assumed that $D = 4$ Fierz transforms in PQQCD commute with the calculation of one-loop corrections. This is not valid in general. However, it is correct in this case, when using the projectors of Ref. [9]. This we have checked by explicit calculation, using the method of Sec. A 1.⁸

Given this result, the PQA-PQB matching can be replaced by matching Q_1^{PQB} regularized in the scheme of Ref. [9] to the *same* operator in the NDR' scheme. It was this latter calculation that was done (correctly) in Refs. [7, 10, 11].

The same result holds true for the operators $Q_{4,5}^{\text{Cont}}$: Fierzing in the PQ theory commutes with calculating the finite correction at one-loop (as long as one uses the same

NDR scheme). Specifically, these operators are exactly matched in PQQCD to

$$Q_4^{\text{PQA}} = 2\left\{[\bar{s}_1^a L d_1^a][\bar{s}_2^b R d_2^b] + [\bar{s}_1^a L d_2^a][\bar{s}_2^b R d_1^b]\right\}, \quad (\text{A46})$$

$$Q_5^{\text{PQA}} = 2\left\{[\bar{s}_1^a \gamma_\mu L d_1^a][\bar{s}_2^b \gamma_\mu R d_2^b] + [\bar{s}_1^a \gamma_\mu L d_2^a][\bar{s}_2^b \gamma_\mu R d_1^b]\right\}, \quad (\text{A47})$$

The claim is that, at one loop, these operators are matched with no finite corrections to

$$Q_4^{\text{PQB}} = 2\left\{[\bar{s}_1^a L d_1^a][\bar{s}_2^b R d_2^b] - \frac{1}{2}[\bar{s}_1^a \gamma_\mu L d_1^b][\bar{s}_2^b \gamma_\mu R d_2^a]\right\}, \quad (\text{A48})$$

$$Q_5^{\text{PQB}} = 2\left\{[\bar{s}_1^a \gamma_\mu L d_1^a][\bar{s}_2^b \gamma_\mu R d_2^b] - 2[\bar{s}_1^a L d_1^b][\bar{s}_2^b R d_2^a]\right\}, \quad (\text{A49})$$

as long as the regularization of Ref. [9] is used in both cases. This was implicitly assumed in Refs. [7, 10, 11]. Because this assumption is correct, the matching calculations done in these works remain valid. We have double-checked this by repeating the calculation from scratch.

This result does *not hold*, however, for $Q_{2,3}^{\text{Cont}}$. Fierzing does not commute with one-loop correcting, even using the same renormalization scheme in both PQA and PQB bases.⁹

Appendix B: Anomalous dimensions

We collect here the anomalous dimensions needed to evolve the B -parameters of Eq. (8) and the golden ratios discussed in Sec. IV B. All anomalous dimensions are in the NDR scheme, with those for the four-fermion operators using the choices of evanescent operators given in Ref. [9].

The two-loop anomalous dimension matrices for $Q_{2,3}^{\text{Cont}}$ operators are calculated in Ref. [9]. (They are the same as for the $Q_{1,2}^{\text{SLL}}$ of that work, since the operators differ only by an overall factor.) For $N_c = 3$ and $N_f = 3$, the results are

$$\gamma_{LL}^{(0)} = \begin{pmatrix} -10 & 1/6 \\ -40 & 34/3 \end{pmatrix}, \quad (\text{B1})$$

$$\gamma_{LL}^{(1)} = \begin{pmatrix} -1237/9 & -37/36 \\ -4580/9 & 557/3 \end{pmatrix}. \quad (\text{B2})$$

The eigenvalues for $\gamma_{LL}^{(0)}$ are 11.0161 and -9.68278 .

For $Q_{4,5}^{\text{Cont}}$, the anomalous dimensions are the same as for $Q_{2,1}^{\text{LR}}$ of Ref. [9]. Taking into account that our ordering

⁸ We stress that this PQA-PQB matching is different from that just discussed for $Q_{2,3}^{\text{Cont}}$ and $Q_{3,3}^{\text{Cont}}$. Here we are using the scheme of Ref. [9] for both bases, while in Secs. A 1 and A 2 we use the scheme of Ref. [9] in the PQA basis and the NDR' scheme in the PQB basis.

⁹ To see this requires an additional calculation from that presented above, since the difference quoted above is due both to the basis change and the change in NDR scheme.

of the operators is opposite to that in Ref. [9], we have

$$\gamma_{LR}^{(0)} = \begin{pmatrix} -16 & 0 \\ 12 & 2 \end{pmatrix}, \quad (\text{B3})$$

$$\gamma_{LR}^{(1)} = \begin{pmatrix} -1207/6 & 201/4 \\ 154 & 49/3 \end{pmatrix}. \quad (\text{B4})$$

The eigenvalues of $\gamma_{LR}^{(0)}$ are -16 and 2 .

The anomalous dimension of the pseudoscalar density (which is the opposite of that of the quark mass) has coefficients [24]

$$\gamma_P^{(0)} = -8, \quad \gamma_P^{(1)} = -\frac{364}{3}. \quad (\text{B5})$$

For the golden combinations, we also need the anomalous dimension of the B_K operator Q_1^{Cont} , which has coefficients [25]

$$\gamma^{(0)} = 4, \quad \gamma^{(1)} = -17/3. \quad (\text{B6})$$

Finally, we can use these results in Eq. (75) to obtain the two-loop anomalous dimensions of the B -parameters themselves. For $B_{2,3}$ we find

$$\gamma_{BLL}^{(0)} = \begin{pmatrix} 6 & 2/5 \\ -50/3 & 82/3 \end{pmatrix}, \quad (\text{B7})$$

$$\gamma_{BLL}^{(1)} = \begin{pmatrix} 947/9 & -37/15 \\ -5725/27 & 1285/3 \end{pmatrix}, \quad (\text{B8})$$

while the results for $B_{4,5}$ are

$$\gamma_{BLR}^{(0)} = \begin{pmatrix} 0 & 0 \\ -18 & 18 \end{pmatrix}, \quad (\text{B9})$$

$$\gamma_{BLR}^{(1)} = \begin{pmatrix} 83/2 & -67/2 \\ -231 & 259 \end{pmatrix}. \quad (\text{B10})$$

Appendix C: Numerical Results for Evolution Kernels

In our numerical simulations we require the evolution kernels to run the B -parameters we evaluate at the lattice scales, $1/a$, to a canonical scale. We use MILC collaboration asqtad ensembles [26] having four nominal lattice spacings. These are labeled C , F , S and U for coarse, fine, superfine and ultrafine, respectively. Strictly speaking, the lattice spacings vary slightly within the coarse

ensembles, and similarly for the fine and superfine ensembles. Here we choose a representative ensemble at each nominal lattice spacing. These are, in the notation of Ref. [3], the C3, F1, S1 and U1 ensembles, all of which have sea quarks in the ratio $m_\ell/m_s = 1/5$. In our numerical work, we evaluate the kernels using the appropriate lattice spacing for each ensemble.

The inverse lattice spacings and corresponding coupling constants are

$$a_C^{-1} = 1.657 \text{ GeV}, \quad \alpha(a_C^{-1}) = 0.3291 \quad (\text{C1})$$

$$a_F^{-1} = 2.342 \text{ GeV}, \quad \alpha(a_F^{-1}) = 0.2734 \quad (\text{C2})$$

$$a_S^{-1} = 3.353 \text{ GeV}, \quad \alpha(a_S^{-1}) = 0.2340 \quad (\text{C3})$$

$$a_U^{-1} = 4.504 \text{ GeV}, \quad \alpha(a_U^{-1}) = 0.2098 \quad (\text{C4})$$

These lattice spacings are obtained from the results for the mass-dependent r_1/a and using $r_1 = 0.3117 \text{ fm}$ [26, 27]. The coupling constants are in the $\overline{\text{MS}}$ scheme, and are obtained using four-loop running as described in Sec. IV A.

We take the canonical final scale to be either 2 GeV , the traditional value, or 3 GeV , which is used, for example, in Ref. [1]. The values of α at these scales are given in Sec. IV A. We calculate the evolution kernel assuming $N_f = 3$, although some of our scales are higher than the charm mass. This is appropriate because our simulations have $N_f = 2 + 1$ flavors of dynamical quarks.

Results for the evolution kernel for the B -parameters, i.e. $W^B(\mu_f, \mu_i)$ of Eq. (74), are given in Tables V, VI and VII. These are obtained using numerical integration of the two-loop RG equations, using the method described in Sec. IV A. The elements of these kernels agree within ~ 0.01 with those obtained using the analytic expressions described in Sec. IV A, and to within ~ 0.02 with those obtained using two-loop running for α .

TABLE V. Results for evolution kernel for B_K , $W_{11}(\mu_f, \mu_i)$. Note that this is the same as the kernel for the operator Q_1^{Cont} .

μ_i	$W_{11}(2 \text{ GeV}, \mu_i)$	$W_{11}(3 \text{ GeV}, \mu_i)$
a_C^{-1}	0.982	0.948
a_F^{-1}	1.014	0.980
a_S^{-1}	1.044	1.008
a_U^{-1}	1.065	1.030

- [1] P. Boyle, N. Garron, and R. Hudspith (RBC Collaboration, UKQCD Collaboration), Phys.Rev. **D86**, 054028 (2012), arXiv:1206.5737 [hep-lat].
[2] V. Bertone *et al.* (ETM), JHEP **1303**, 089 (2013), arXiv:1207.1287 [hep-lat].
[3] T. Bae *et al.* (SWME Collaboration), (2013),

- arXiv:1309.2040 [hep-lat].
[4] N. Carrasco *et al.* (ETM collaboration), (2013), arXiv:1310.5461 [hep-lat].
[5] T. Bae, Y.-C. Jang, H. Jeong, J. Kim, J. Kim, *et al.*, (2013), arXiv:1310.7372 [hep-lat].
[6] A. Lytle, P. Boyle, N. Garron, R. Hudspith, and

TABLE VI. Evolution matrices, $W_{LL}^B(\mu_f, \mu_i)$, for B -parameters of LL operators $\{B_2, B_3\}$.

μ_i	$W_{LL}^B(2 \text{ GeV}, \mu_i)$	$W_{LL}^B(3 \text{ GeV}, \mu_i)$
a_C^{-1}	$\begin{pmatrix} 0.956 & -0.001 \\ 0.010 & 0.822 \end{pmatrix}$	$\begin{pmatrix} 0.885 & -0.003 \\ 0.224 & 0.584 \end{pmatrix}$
a_F^{-1}	$\begin{pmatrix} 1.033 & 0.001 \\ -0.090 & 1.154 \end{pmatrix}$	$\begin{pmatrix} 0.956 & -0.002 \\ 0.101 & 0.821 \end{pmatrix}$
a_S^{-1}	$\begin{pmatrix} 1.100 & 0.005 \\ -0.316 & 1.522 \end{pmatrix}$	$\begin{pmatrix} 1.018 & 0.001 \\ -0.048 & 1.083 \end{pmatrix}$
a_U^{-1}	$\begin{pmatrix} 1.147 & 0.008 \\ -0.519 & 1.840 \end{pmatrix}$	$\begin{pmatrix} 1.063 & 0.003 \\ -0.186 & 1.310 \end{pmatrix}$

TABLE VII. Evolution matrices, $W_{LR}^B(\mu_f, \mu_i)$, for B -parameters of LR operators $\{B_4, B_5\}$.

μ_i	$W_{LR}^B(2 \text{ GeV}, \mu_i)$	$W_{LR}^B(3 \text{ GeV}, \mu_i)$
a_C^{-1}	$\begin{pmatrix} 0.994 & 0.005 \\ 0.114 & 0.882 \end{pmatrix}$	$\begin{pmatrix} 0.986 & 0.011 \\ 0.281 & 0.710 \end{pmatrix}$
a_F^{-1}	$\begin{pmatrix} 1.004 & -0.004 \\ -0.094 & 1.097 \end{pmatrix}$	$\begin{pmatrix} 0.995 & 0.004 \\ 0.116 & 0.881 \end{pmatrix}$
a_S^{-1}	$\begin{pmatrix} 1.013 & -0.011 \\ -0.304 & 1.312 \end{pmatrix}$	$\begin{pmatrix} 1.002 & -0.002 \\ -0.051 & 1.053 \end{pmatrix}$
a_U^{-1}	$\begin{pmatrix} 1.019 & -0.016 \\ -0.473 & 1.485 \end{pmatrix}$	$\begin{pmatrix} 1.007 & -0.006 \\ -0.186 & 1.191 \end{pmatrix}$

C. Sachrajda (the RBC-UKQCD Collaboration), (2013), arXiv:1311.0322 [hep-lat].

[7] J. Kim, W. Lee, and S. R. Sharpe, Phys.Rev. **D83**,

094503 (2011), arXiv:1102.1774 [hep-lat].

- [8] R. Gupta, T. Bhattacharya, and S. R. Sharpe, Phys.Rev. **D55**, 4036 (1997), arXiv:hep-lat/9611023 [hep-lat].
- [9] A. J. Buras, M. Misiak, and J. Urban, Nucl.Phys. **B586**, 397 (2000), arXiv:hep-ph/0005183 [hep-ph].
- [10] S. R. Sharpe and A. Patel, Nucl.Phys. **B417**, 307 (1994), arXiv:hep-lat/9310004 [hep-lat].
- [11] W.-j. Lee and S. R. Sharpe, Phys.Rev. **D68**, 054510 (2003), arXiv:hep-lat/0306016 [hep-lat].
- [12] D. H. Adams and W. Lee, Phys.Rev. **D75**, 074502 (2007), arXiv:hep-lat/0701014 [hep-lat].
- [13] D. Becirevic and G. Villadoro, Phys.Rev. **D70**, 094036 (2004), arXiv:hep-lat/0408029 [hep-lat].
- [14] J. A. Bailey, H.-J. Kim, W. Lee, and S. R. Sharpe, Phys.Rev. **D85**, 074507 (2012), arXiv:1202.1570 [hep-lat].
- [15] F. Gabbiani, E. Gabrielli, A. Masiero, and L. Silvestrini, Nucl.Phys. **B477**, 321 (1996), arXiv:hep-ph/9604387 [hep-ph].
- [16] S. R. Sharpe, A. Patel, R. Gupta, G. Guralnik, and G. W. Kilcup, Nucl.Phys. **B286**, 253 (1987).
- [17] G. Kilcup, R. Gupta, and S. R. Sharpe, Phys. Rev. **D57**, 1654 (1998), arXiv:hep-lat/9707006.
- [18] A. J. Buras and J. Gierbach, JHEP **1203**, 052 (2012), arXiv:1201.1302 [hep-ph].
- [19] J. Kim, W. Lee, and S. R. Sharpe, Phys.Rev. **D81**, 114503 (2010), arXiv:1004.4039 [hep-lat].
- [20] A. J. Buras, Rev.Mod.Phys. **52**, 199 (1980).
- [21] K. Chetyrkin, B. A. Kniehl, and M. Steinhauser, Phys.Rev.Lett. **79**, 2184 (1997), arXiv:hep-ph/9706430 [hep-ph].
- [22] F. Mescia and J. Virto, Phys.Rev. **D86**, 095004 (2012), arXiv:1208.0534 [hep-ph].
- [23] A. Patel and S. R. Sharpe, Nucl.Phys. **B395**, 701 (1993), arXiv:hep-lat/9210039 [hep-lat].
- [24] R. Tarrach, Nucl.Phys. **B183**, 384 (1981).
- [25] A. J. Buras and P. H. Weisz, Nucl.Phys. **B333**, 66 (1990).
- [26] A. Bazavov, D. Toussaint, C. Bernard, J. Laiho, C. DeTar, *et al.*, Rev.Mod.Phys. **82**, 1349 (2010), arXiv:0903.3598 [hep-lat].
- [27] C. Bernard, private communications (2009-13).